

The performance of improved H-modes at ASDEX Upgrade and projection to ITER

George Sips

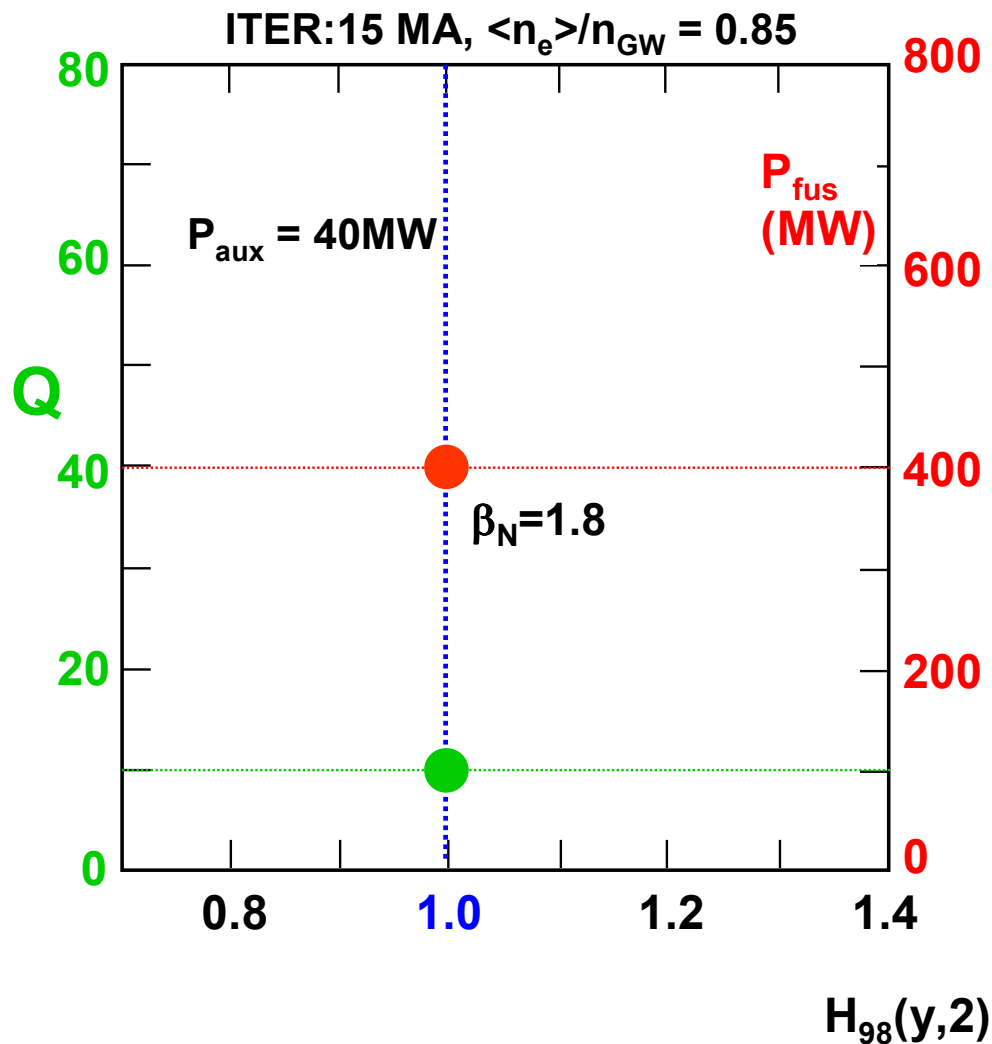
MPI für Plasmaphysik, EURATOM-Association, D-85748, Germany

*G. Tardini¹, C. Forest², O. Gruber¹, P. Mc Carthy³, A. Gude¹, L.D. Horton¹, V. Igochine¹, O. Kardaun¹,
C.F. Maggi¹, M. Maraschek¹, V. Mertens¹, R. Neu¹, A. Peeters¹, G. V. Pereverzev¹, A. Stäbler¹, J. Stober¹,
W. Suttrop¹ and the ASDEX Upgrade Team.*

¹ *Max-Planck-Institut für Plasmaphysik, EURATOM-Association, D-85748, Germany.*

² *The University of Wisconsin, Madison, USA.*

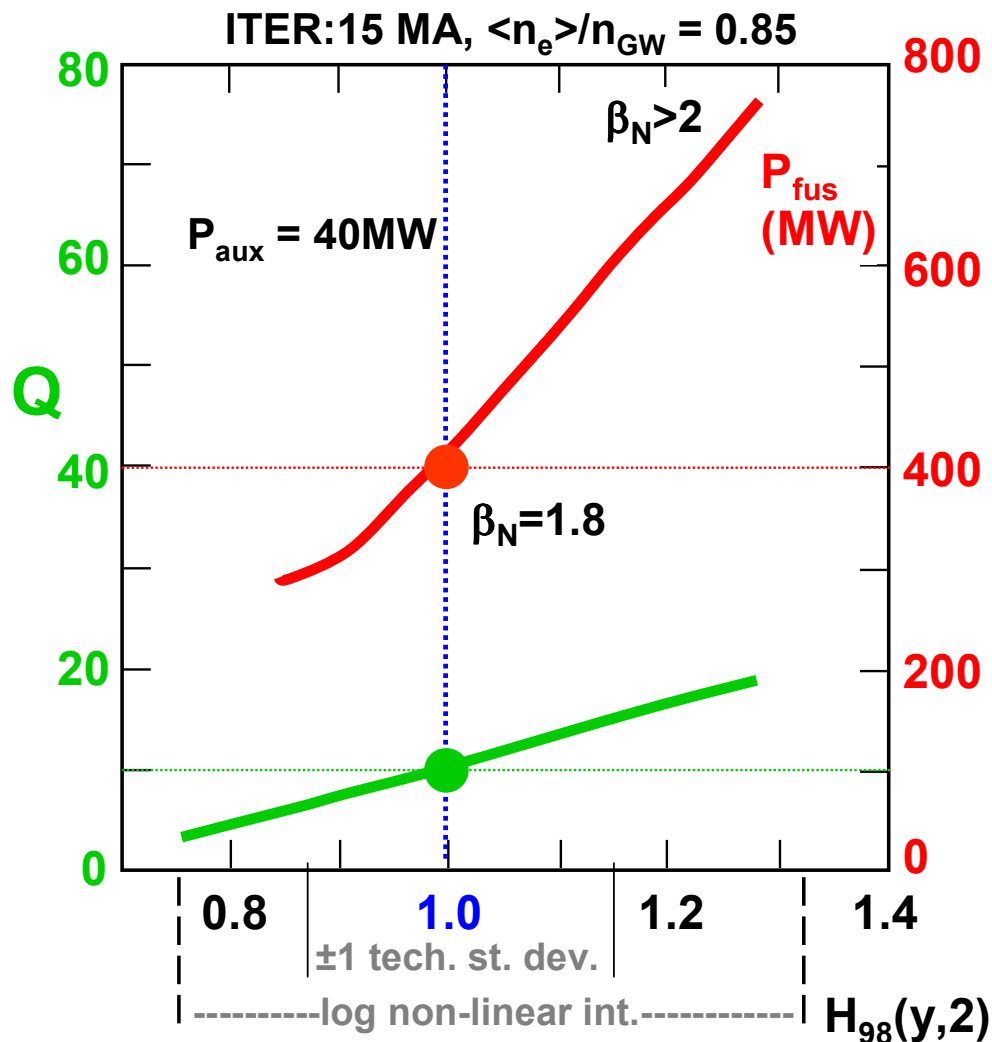
³ *Dep. of Physics, University College Cork, Association EURATOM-DCU, Cork, Ireland.*



ITER primary goal:
 $Q=10$, $P_{fus} \sim 400\text{MW}$.

Energy confinement:
 IPB98(y,2) scaling expression.

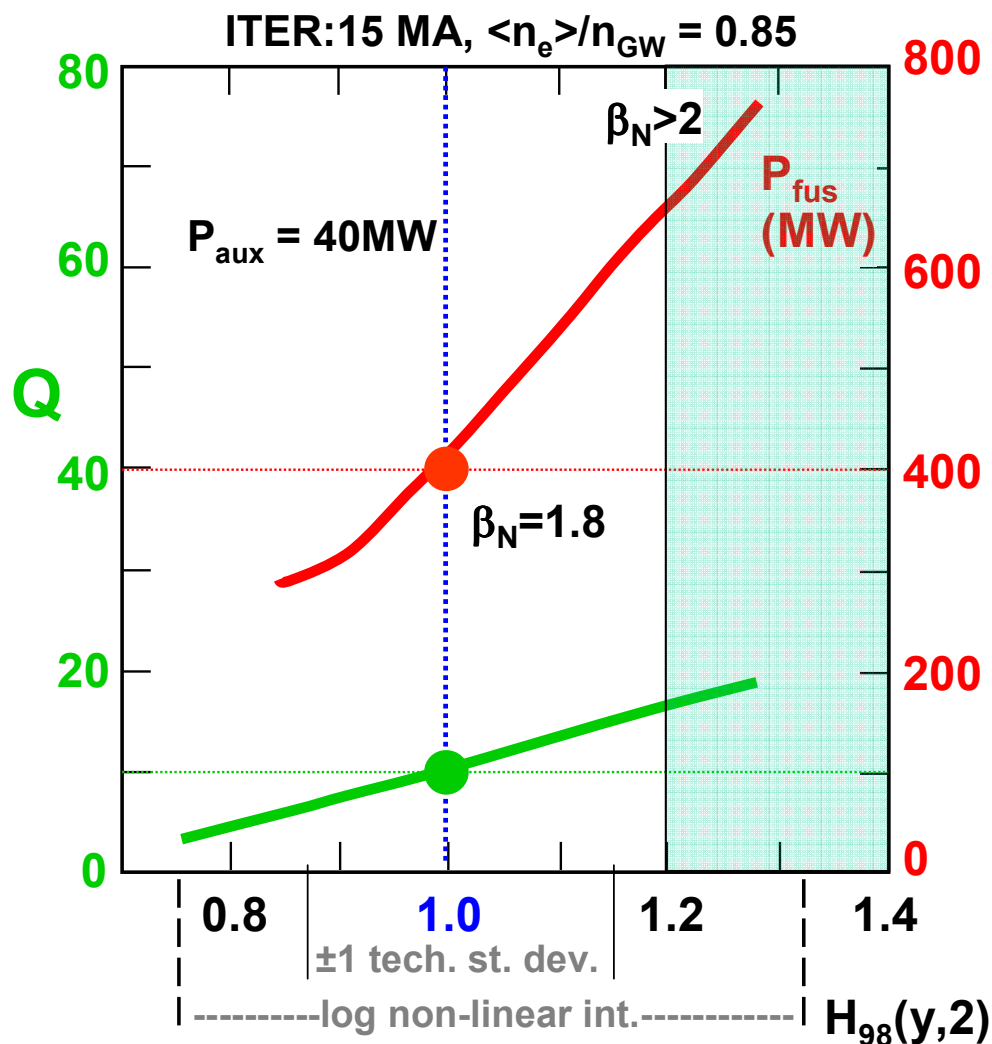
→ ITER size, 15MA/5.3T,
 $P_{aux} \leq 73\text{ MW}$, $\langle n_e \rangle = 0.85$,.....



Integrated simulation codes: →
 ‘envelope’ of performance.

- Strong dependence, of Q and P_{fus} with $H_{98}(y,2)$.

Significant increase in ITER performance for ‘small’ increase in energy confinement.



Integrated simulation codes: →
‘envelope’ of performance.

- Strong dependence, of Q and P_{fus} with $H_{98}(y,2)$.

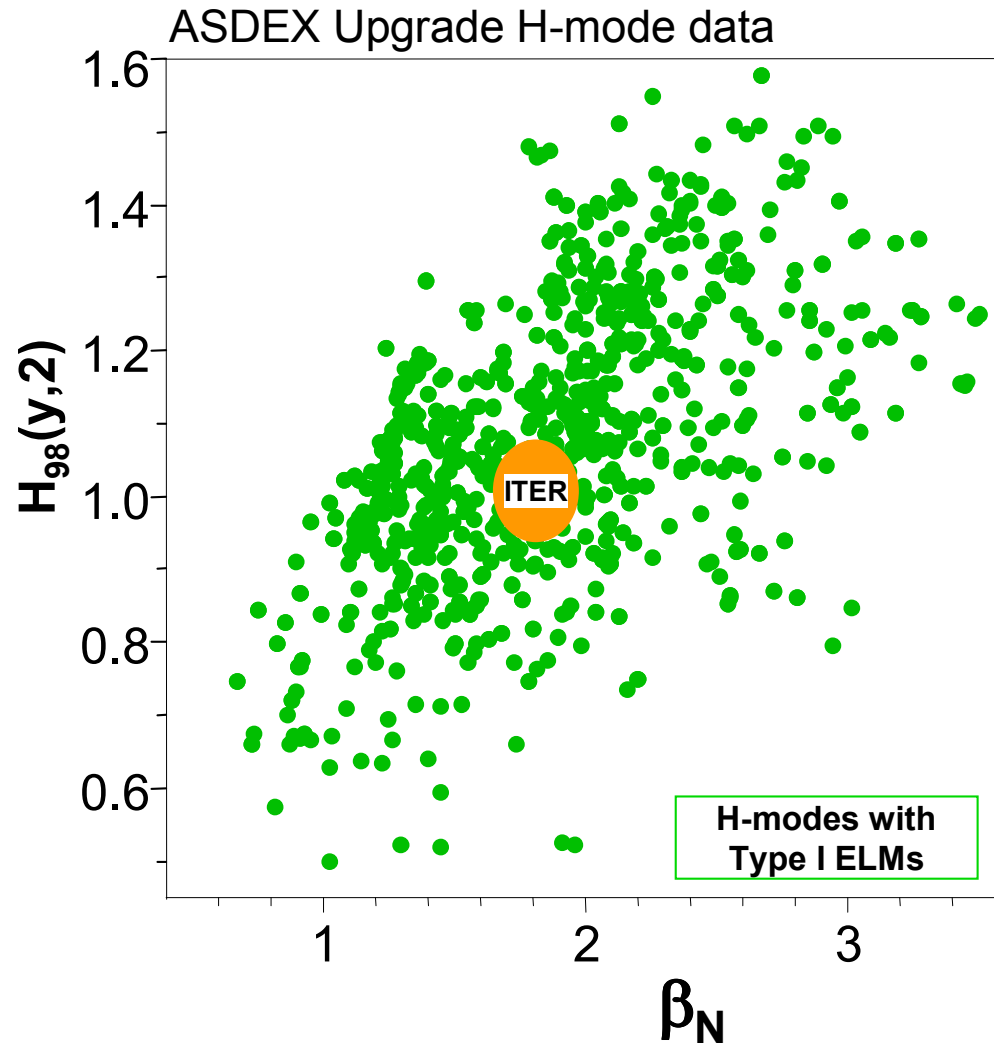
Significant increase in ITER performance for ‘small’ increase in energy confinement.

$H_{98}(y,2) > 1$, and $\beta_N > 2$:

- Higher performance at 15 MA.
- Long pulse operation, $I_p = 11$ to 14 MA, with $Q = 5-10$ (Hybrid).
- DEMO: $H_{98}(y,2) \geq 1.2$, $\beta_N \geq 3.5$.

Mukhovatov V. et al Nucl. Fusion 43 (2003) 942

- **ASDEX Upgrade:**
Improved H-modes ($H_{98}(y,2) > 1$, and $\beta_N > 2$).
- **Operational range:**
 - wide range in density, T_{i0}/T_{e0} and v^* .
 - at $q_{95} \rightarrow 3.1$.
 - high beta: Limits and control of NTMs.
- **Scaling to ITER using experimental data.**
- **Conclusions.**

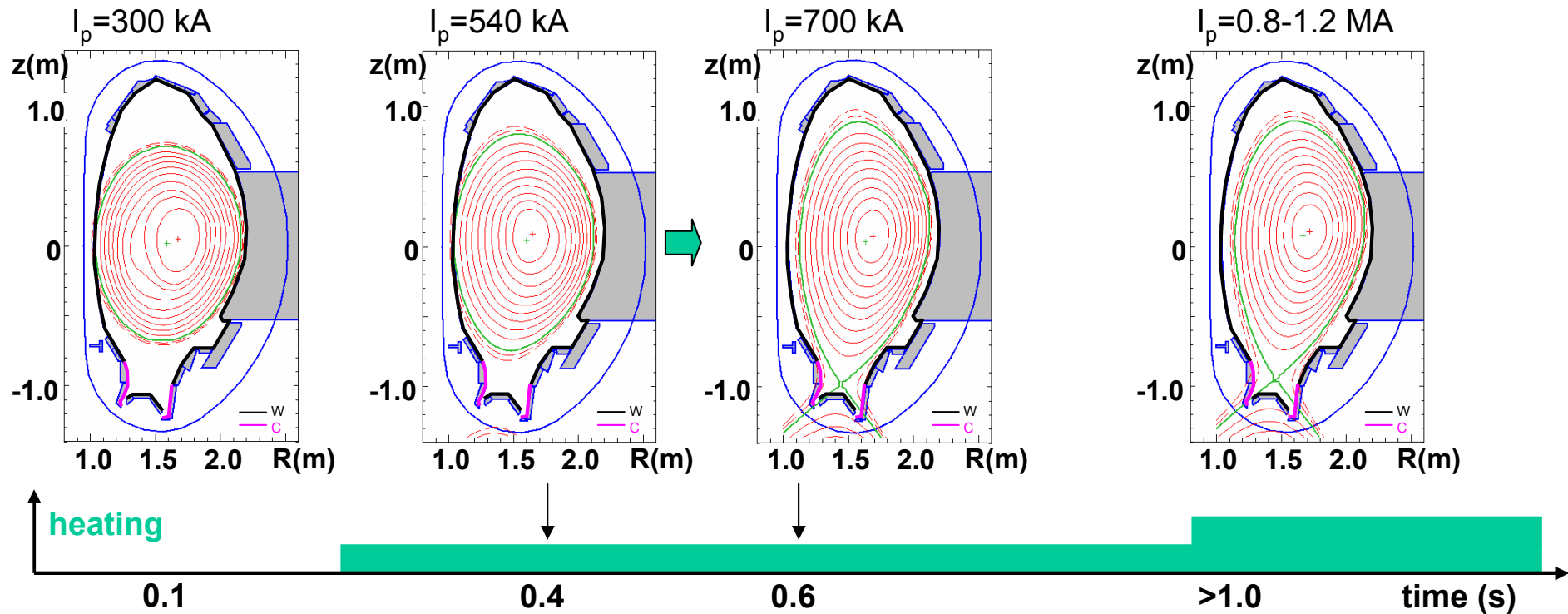


H-mode operation for a wide range of plasma conditions:

- $I_p=0.6-1.4\text{MA}$, $B_T=1.6-3.0\text{T}$.

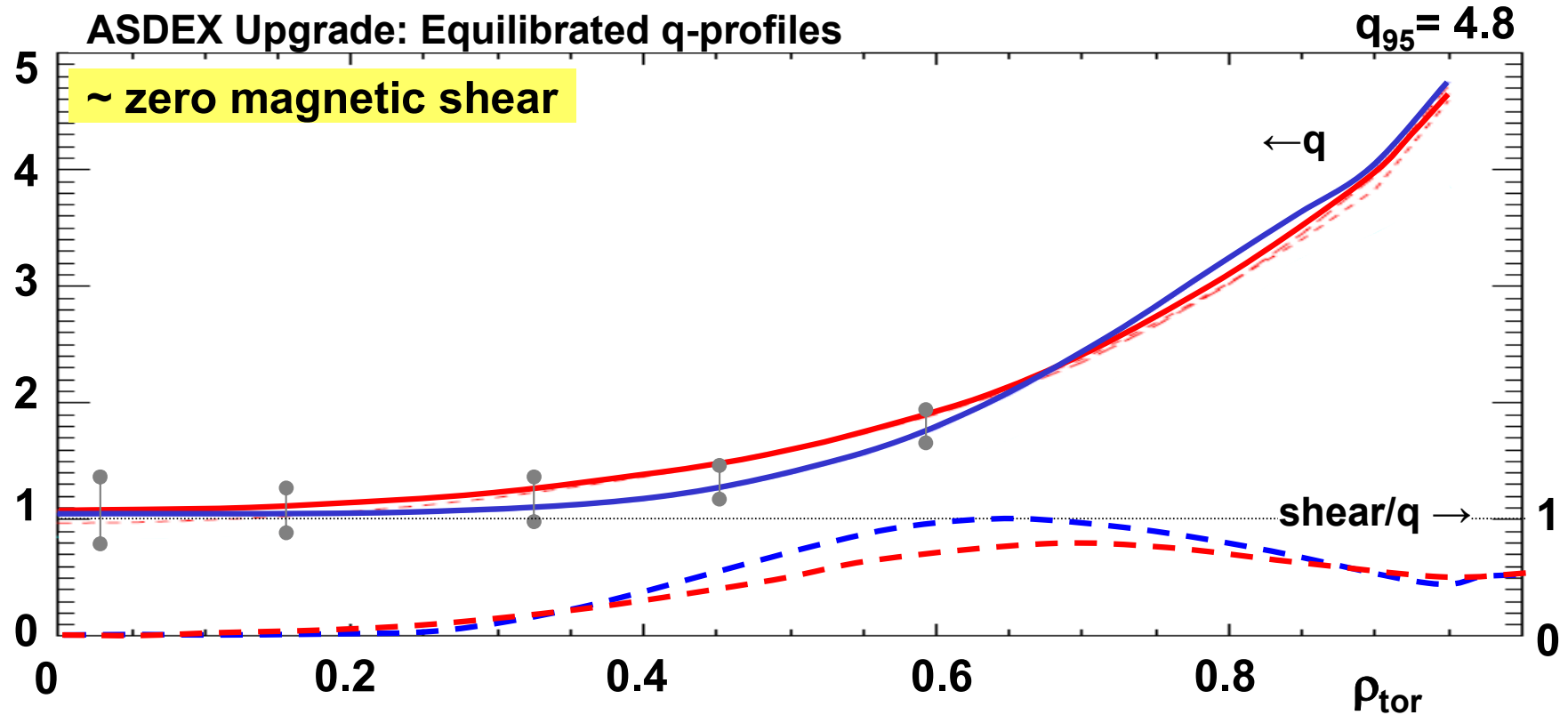
All type I ELMy H-modes:

- $q_{95} < 5.5$, stationary > 0.2 s.
(values shown are averaged)

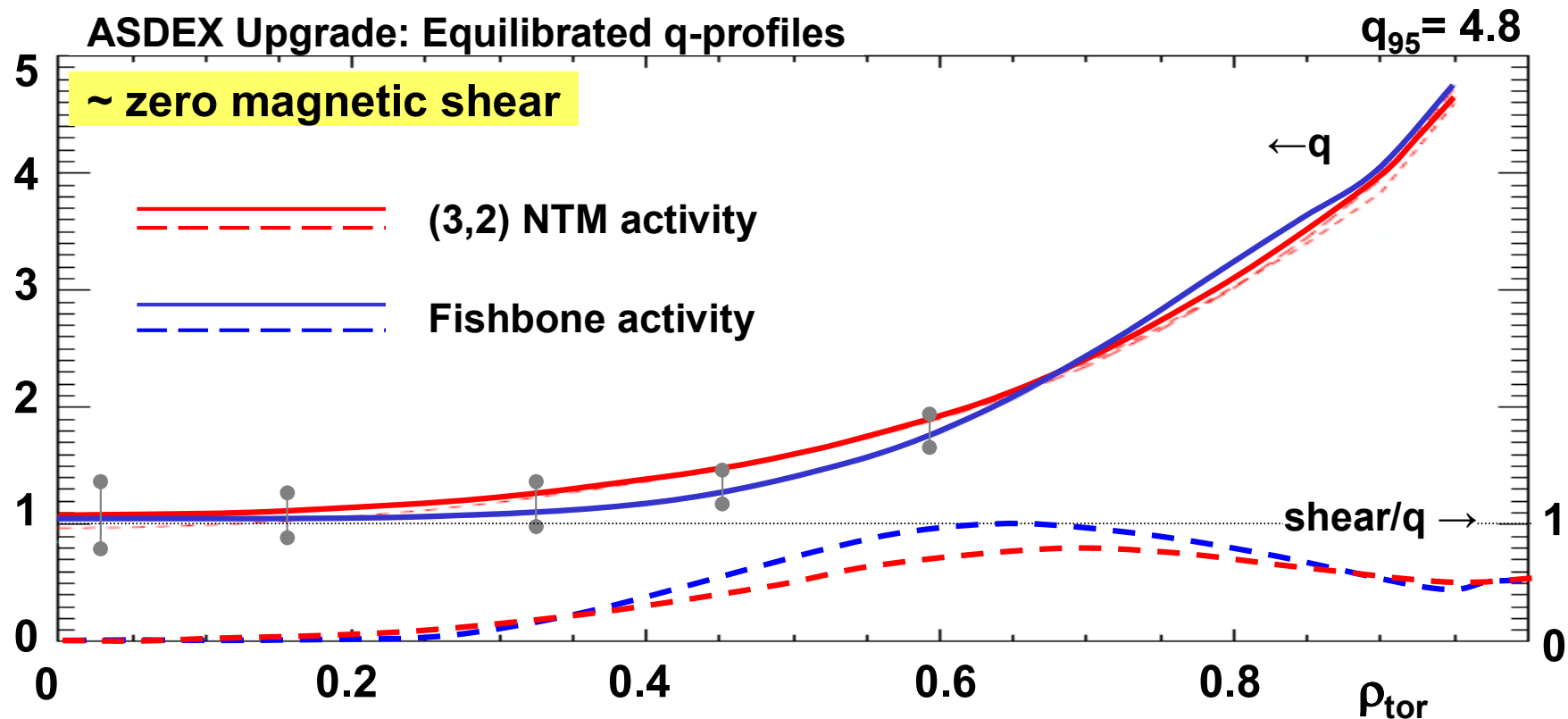


- Current rise:**
1. Early divertor configuration $t \sim 0.5$ s.
 2. → low $\langle n_e \rangle \sim 3 \times 10^{19} \text{ m}^{-3}$, control of impurities.
 3. Additional heating: Slow down the current penetration.

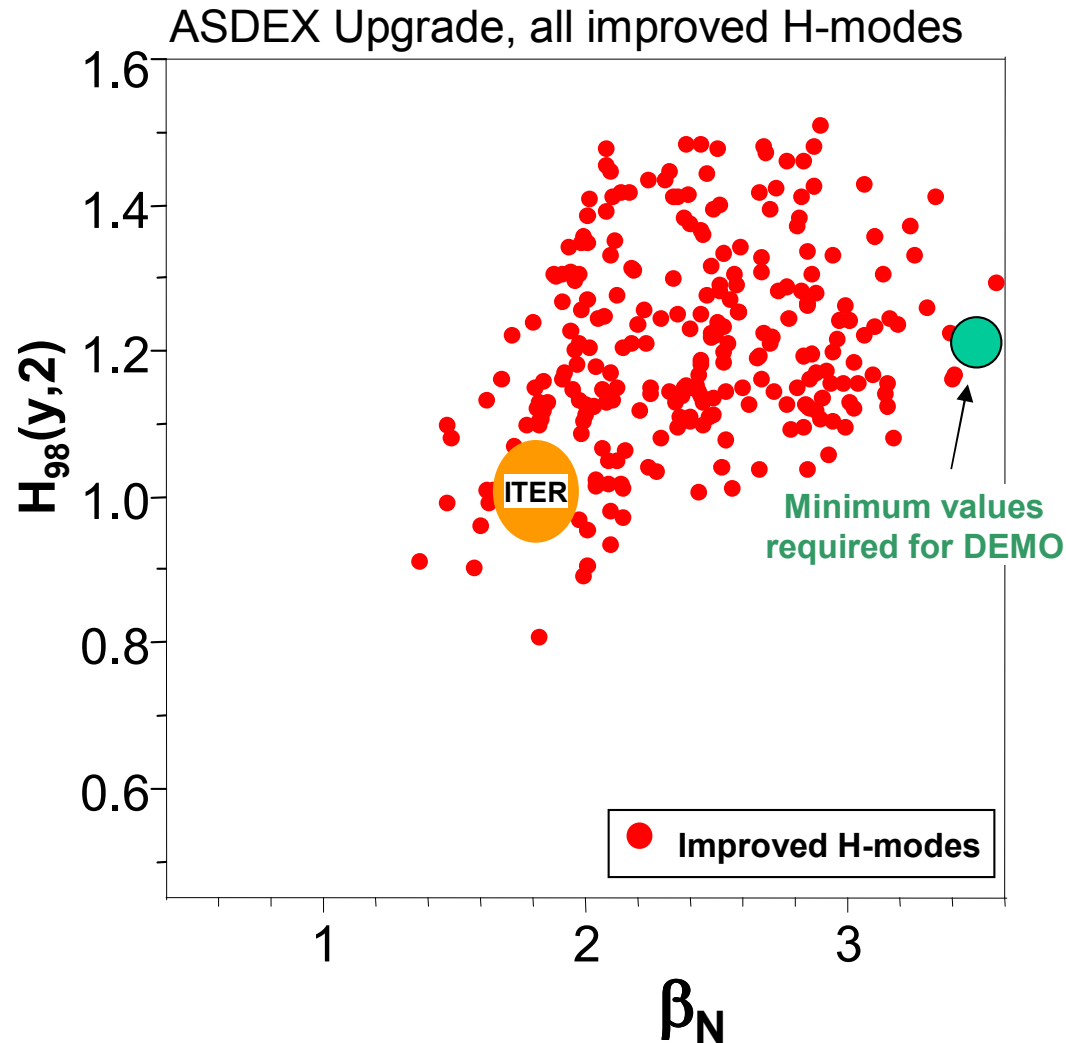
→ Low magnetic shear in the centre.



- MSE data available in 2006. *McCarthy P. et al, EX/P3-7*
- Timing of preheating: 'control' of q-profile $\rightarrow H_{98}(y,2)$. *Stober J. et al, EX/P1-7*
- The q-profile remains flat in the core.

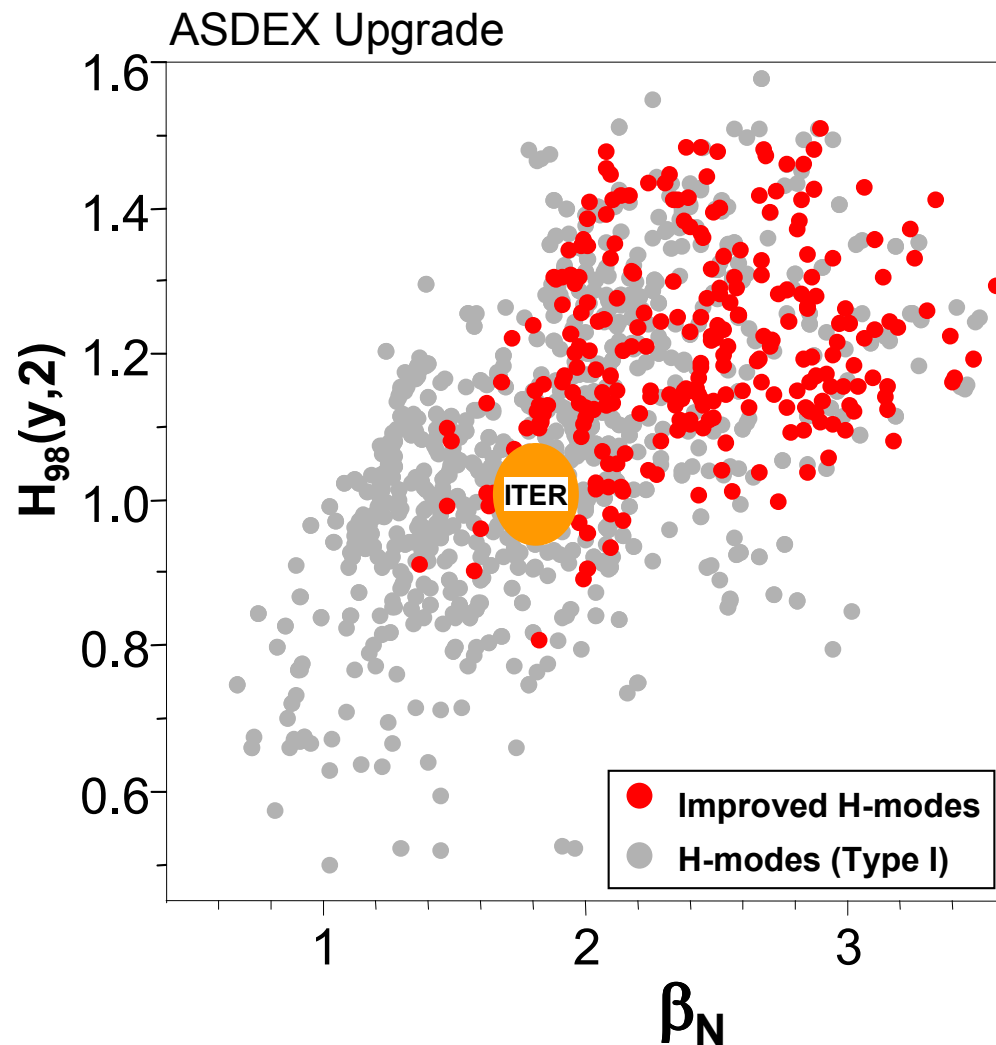


- MSE data available in 2006.
- Timing of preheating: 'control' of q-profile \rightarrow $H_{98}(y,2)$.
- The q-profile remains flat in the core. **MHD modes main candidate.**
Typically (3,2) NTMs and higher (m,n) activity or fishbone activity.



A second dataset includes all “improved H-mode” discharges:

- **Early heating** (some selected cases with late heating).
- Stationary for > 0.5 s.
- NOT just a selection of the best discharges.



Improved H-modes do not exclusively occupy the domain $H_{98}(y,2) > 1$ at $\beta_N = 2-3$.

Any H-mode, when it manages to achieve high beta is likely to develop low central shear in the centre, due to bootstrap current (overlap of 'grey' and 'red' data).

Physics criteria for improved H-modes would depend on the details of the current density profile (not routinely available).

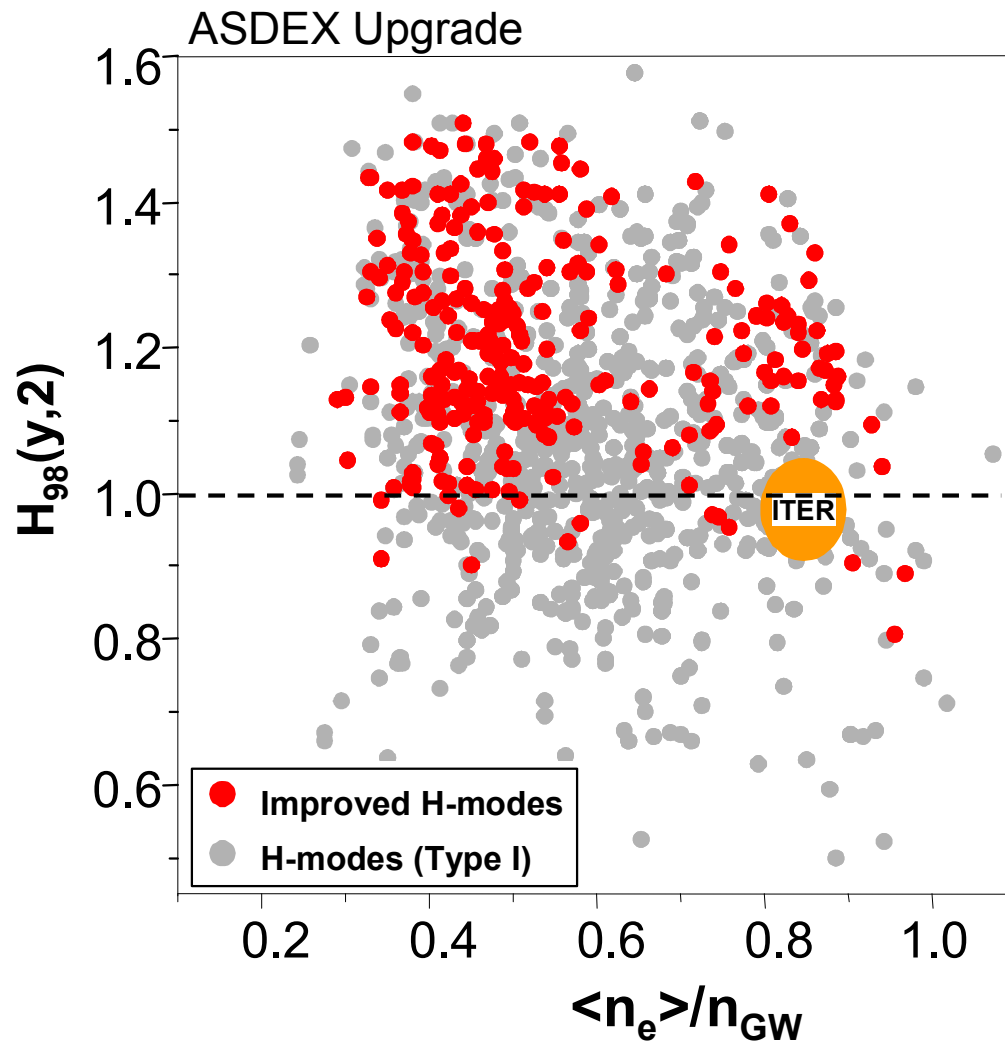
Average values	Type I ELMy H-modes (944)	Improved H-modes (259)
q_{95}	4.1	4.0
$H_{98}(y,2)$	1.08	1.21
β_N	1.89	2.43
I_i	0.95	0.89

Various physics studies on the reason for the high stability/ confinement in improved H-modes.

Core: *Stober J. et al, EX/P1-7*

Pedestal: *Suttrop W. et al, EX/8-5*
Maggi C. et al, IT/P1-6
(various experiments)

Similar results have been obtained in other experiments (DIII-D, JET, JT-60U, NSTX..), for a range of conditions (See this conference !!).



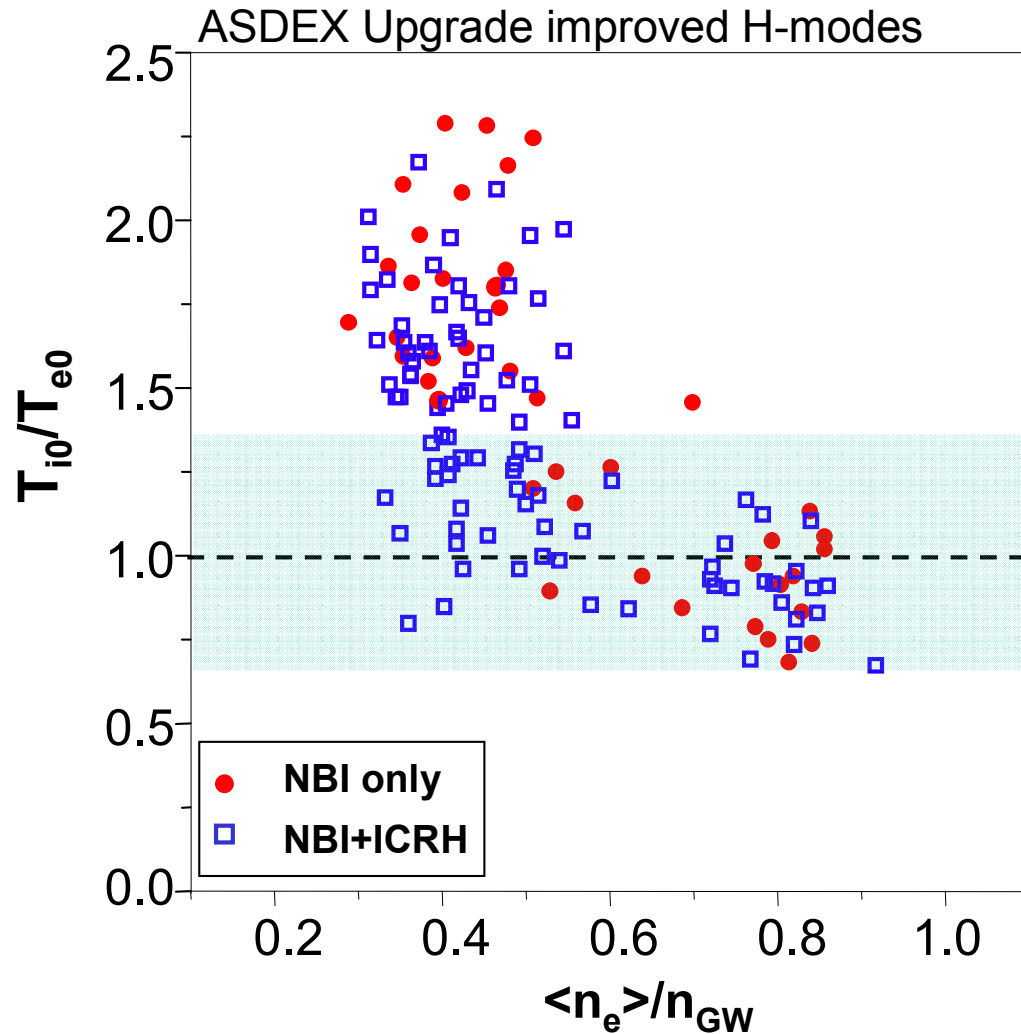
Improved H-modes:
Typically operate at low density,
 $\langle n_e \rangle / n_{GW} = 0.35-0.6$.

After formation of $q(r)$, the
density can be increased
together with an increase in
heating power and δ .

$\langle n_e \rangle / n_{GW} = 0.85$, $H_{98}(y,2) \sim 1.2$
are obtained at high $\delta=0.4$.

→ At 1MA: $\langle n_e \rangle = 1.1 \times 10^{20} \text{ m}^{-3}$.

→ Tolerable ELMs.

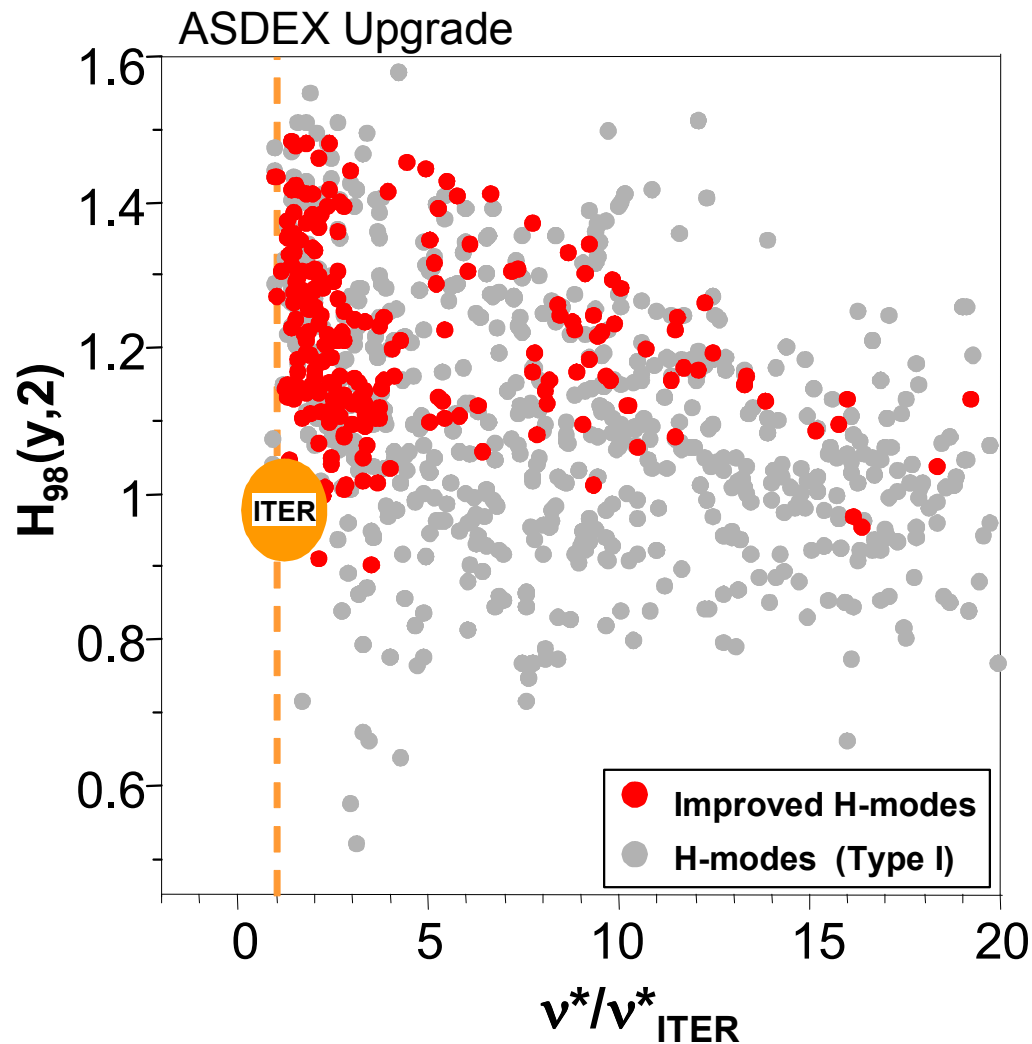


1. Operation at high $\langle n_e \rangle$.
2. ICRH and NBI at low $\langle n_e \rangle$.

$$\rightarrow 0.7 < T_{i0}/T_{e0} < 2.5$$

$T_{i0}/T_{e0} \sim 1$ for a substantial subset of the data, while maintaining high confinement.

Moreover, some of these discharges have low plasma rotation (low momentum input).



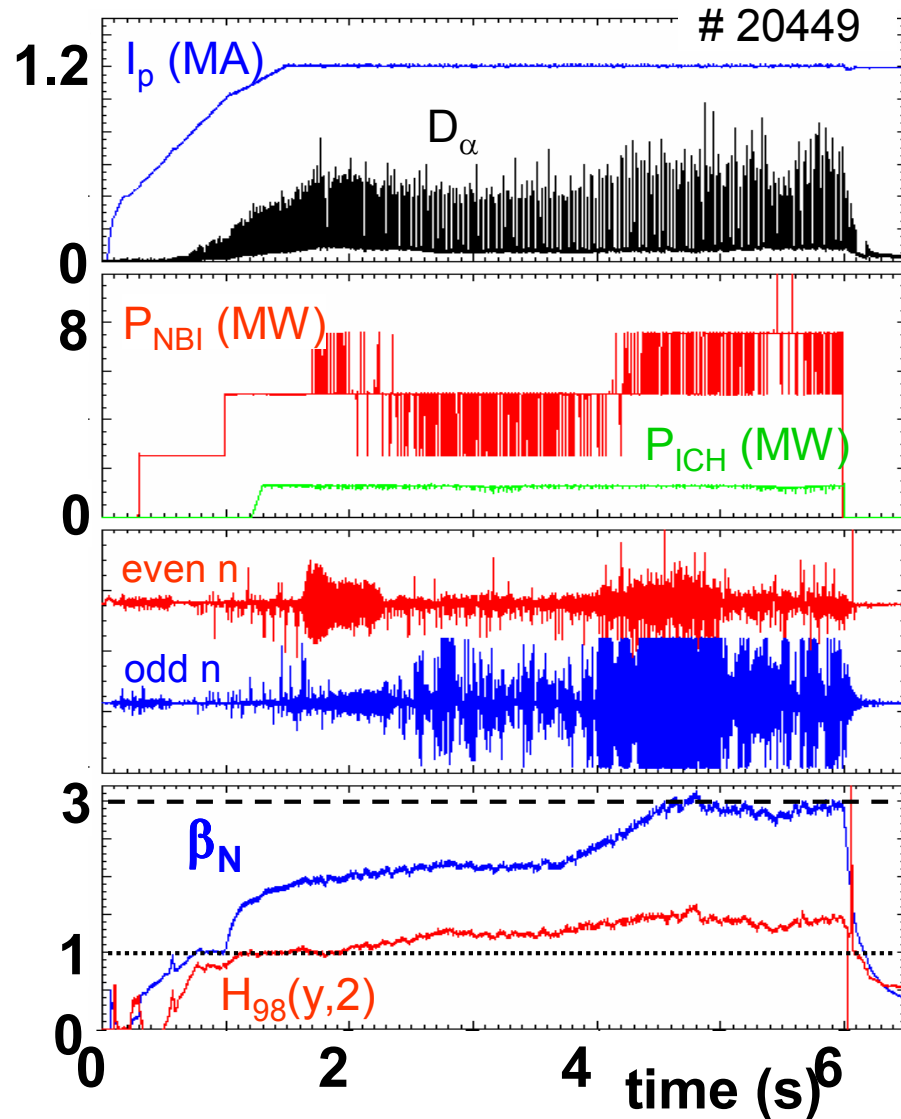
Strongest correlation of maximum $H_{98}(y,2)$ with plasma collisionality (v^*/v^*_{ITER}).

Also density peaking ($n_{e0}/\langle n_e \rangle$) can be higher at lower v^*/v^*_{ITER} .

Weisen H. et al, EX/8-4

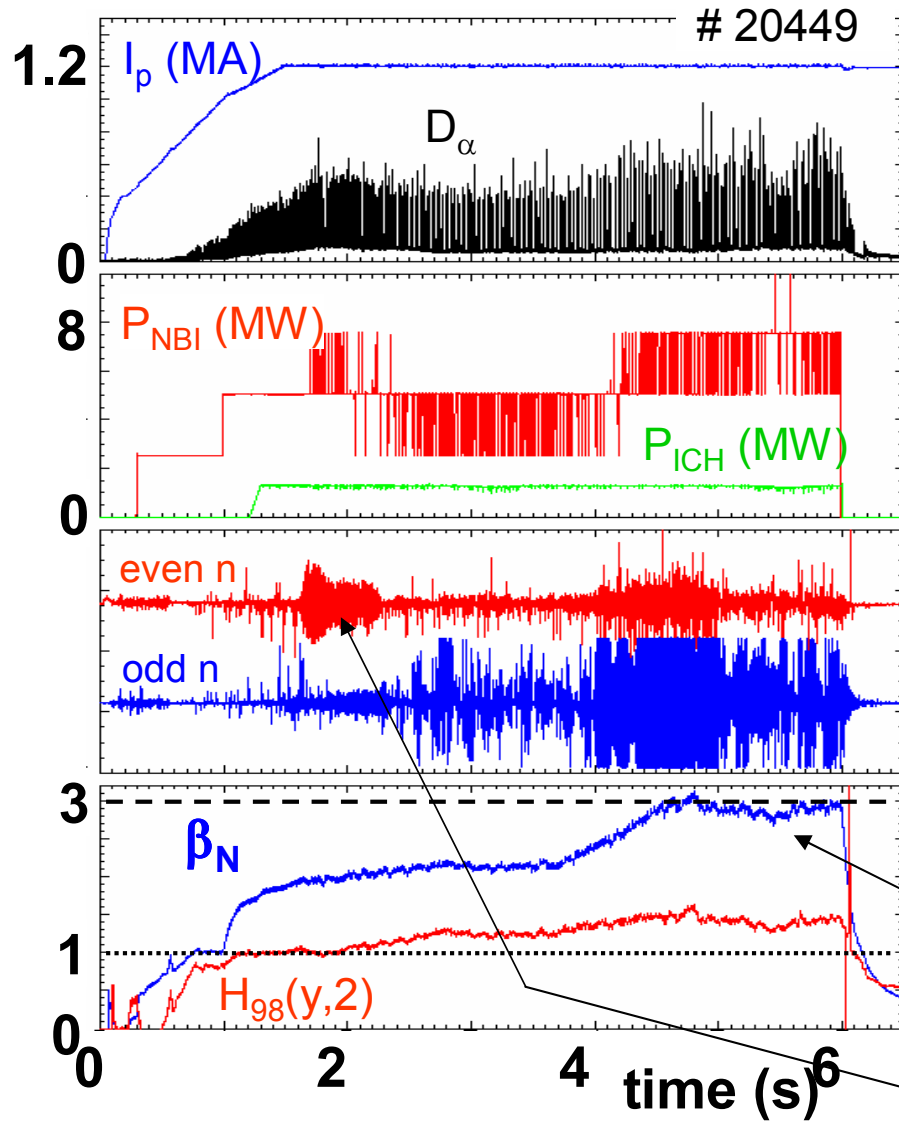
→ β and v^* dependence of the IPB98($y,2$) scaling expression are under investigation.

McDonald D. et al, EX/P3-5



$1.2\text{MA}/2.0\text{T} \rightarrow q_{95} = 3.17,$

- NBI used with beta feedback, 50% of NBI is off-axis!
Central ICRF heating.
- $\langle n_e \rangle = 6.4 \times 10^{19} \text{m}^{-3}$, $T_{i0}/T_{e0} = 1.4$
 $\langle n_e \rangle / n_{\text{GW}} = 0.42$, $v^*/v^*_{\text{ITER}} = 2.$
- $H_{98}(y,2)$ rises to 1.4 at $\beta_N = 2.9.$
- $C_{W,\text{core}} = 2.5 \times 10^{-5}$ ($< 10^{-4}$).



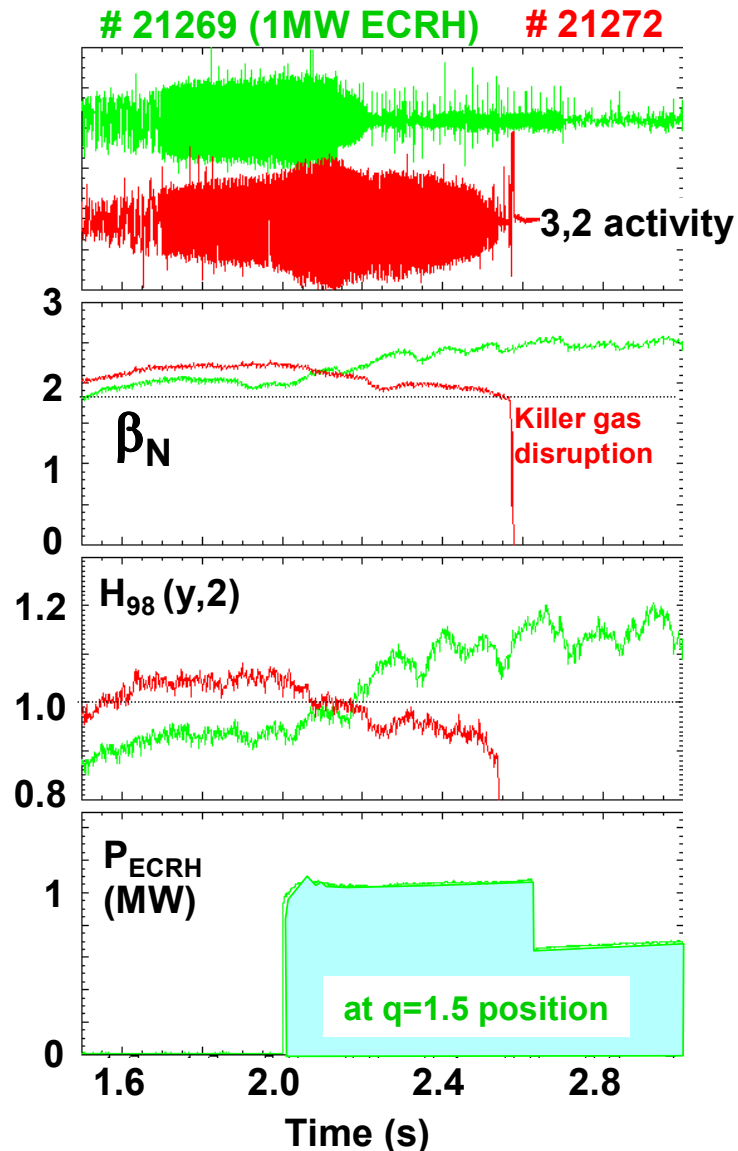
$1.2\text{MA}/2.0\text{T} \rightarrow q_{95} = 3.17,$

- NBI used with beta feedback, 50% of NBI is off-axis. Central ICRF heating.
- $\langle n_e \rangle = 6.4 \times 10^{19} \text{m}^{-3}$, $T_{i0}/T_{e0} = 1.4$
 $\langle n_e \rangle / n_{\text{GW}} = 0.42$, $v^*/v_{\text{ITER}}^* = 2$.
- $H_{98}(y,2)$ rises to 1.4 at $\beta_N = 2.9$.
- $C_{W,\text{core}} = 2.5 \times 10^{-5}$ ($< 10^{-4}$).

Core MHD:

- (1,1) fishbones.
- (4,3) NTMs.
- NO sawteeth.

Early (3,2) NTM when $\beta_N \sim 2$.



1. ECCD: Stabilise this (3,2) NTM at $q_{95} \sim 3.1$
 After ECCD, discharge continues as improved H-mode (shown before).

Zohm H. et al, EX/4-1Rb

2. Otherwise (2,1) NTM may develop, and disruption recognition algorithms will act: (mode-lock, radiation peaking, regime identification, neural net):

- React by issuing a soft stop or triggering killer gas injection.

Pautasso G. et al, EX/P8-7

3. Stabilisation of (3,2) NTM is not required for improved H-modes with $q_{95} > 4$.

Stober J. et al, EX/P1-7

Motivation:

- Integrated simulation codes rely on use of transport models and models for actuators, require benchmarking on current experiments.
- **Scaling the measured kinetic profiles to ITER:** 100% fit to experimental data, gradient length preserved, pedestal.
 - Use experimental profile shapes.
 - Same β_N , H-factor's.
 - Use ITER geometry.
 - Impurities: Be 2 %, Ar 0.12 %, He 4.3 % $\rightarrow (n_D+n_T)/n_e \sim 0.8$.

Luce T. et al 2004 Phys. Plasmas 11 2627

Assemble set of discharges with good profile measurements.

ITER predictions: P_{fus} , P_{aux} , Q (+ other parameters using ASTRA).

Tardini G. et al 33rd EPS Conference, Rome 19-23 June 2006, P1.112

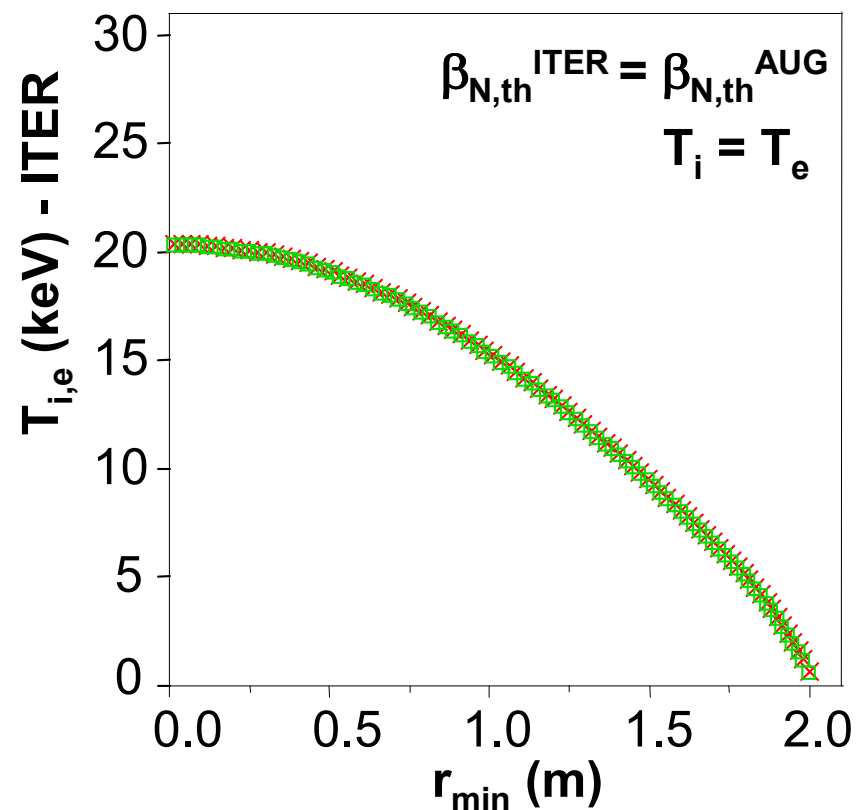
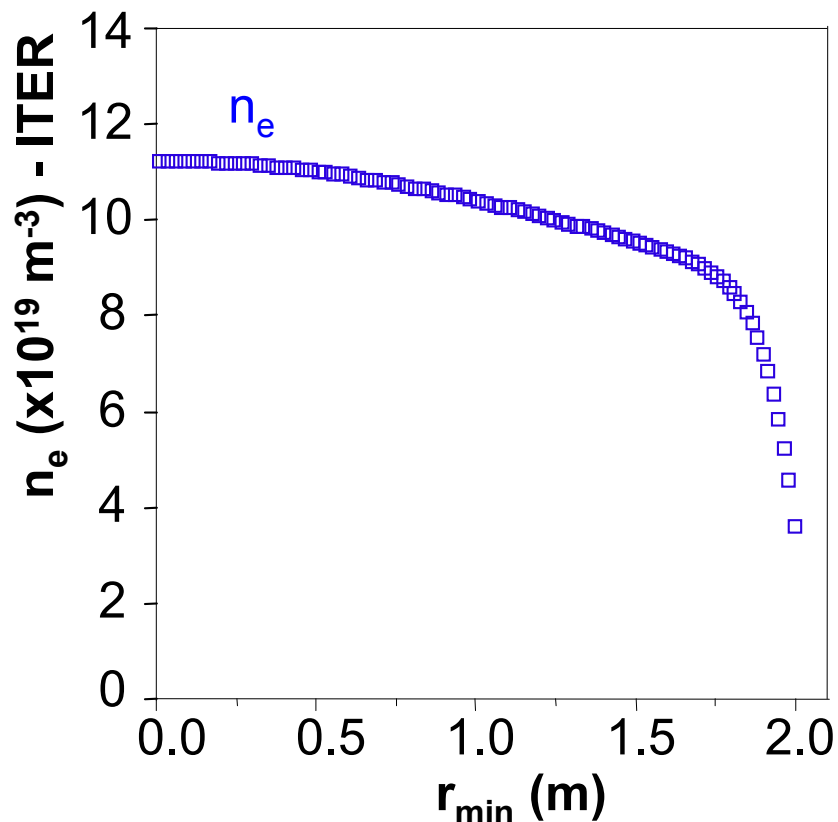


Scaling to ITER using experimental data



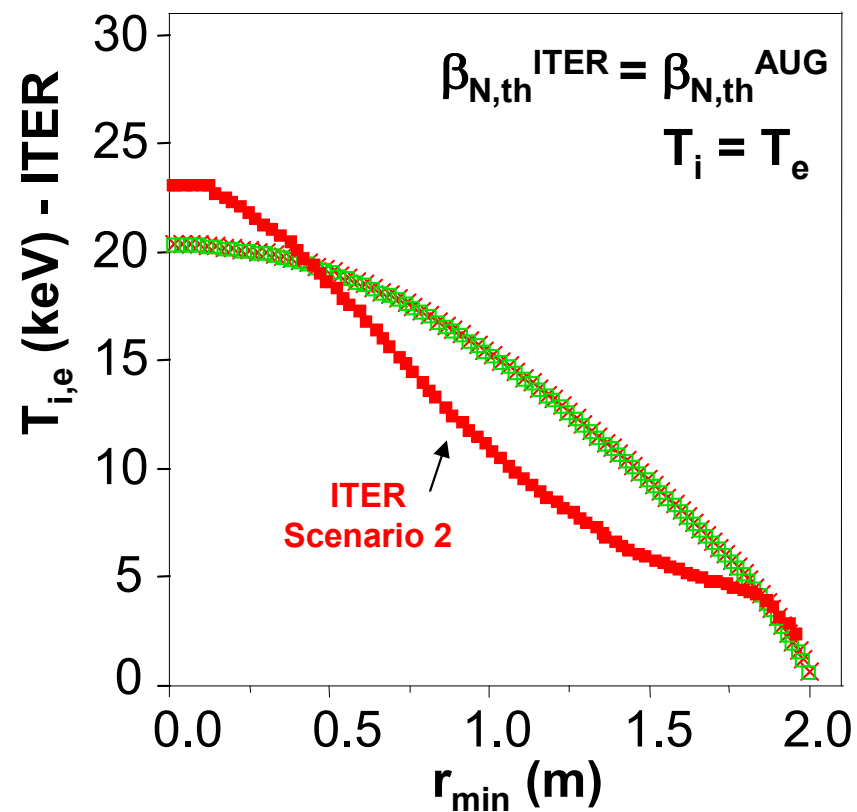
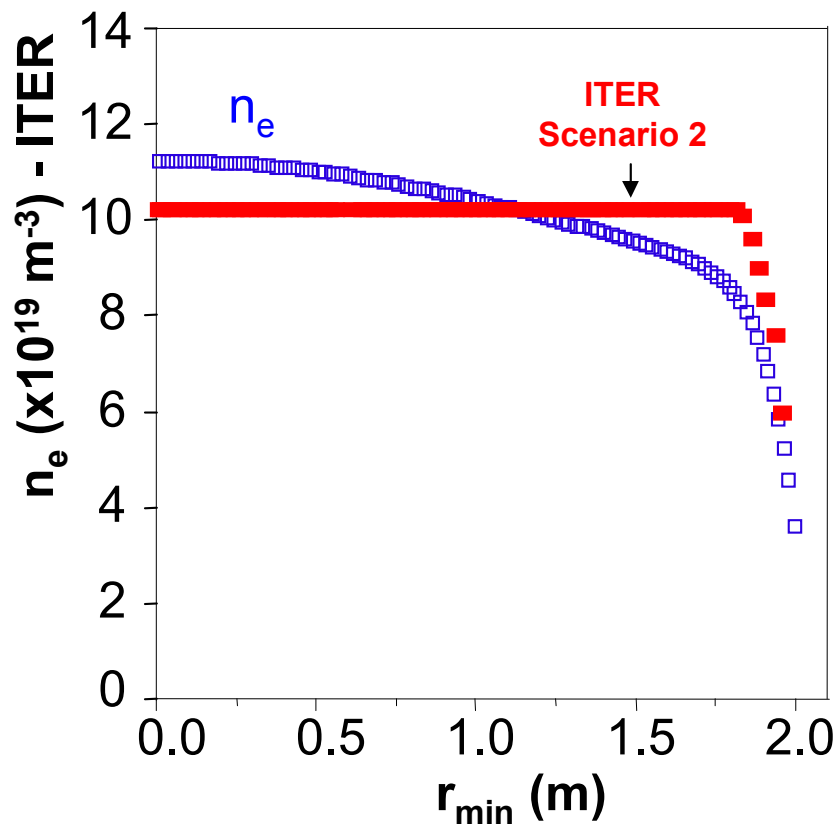
Density: Use shape of n_e profile from ASDEX Upgrade, **set $\langle n_e \rangle = 0.85n_{GW}$.**

Temperatures: Use shape of T_i profile or use shape of T_e profile from ASDEX Upgrade (select highest), **set $T_i = T_e$ and $\beta_N^{ITER} = \beta_N^{AUG}$.**



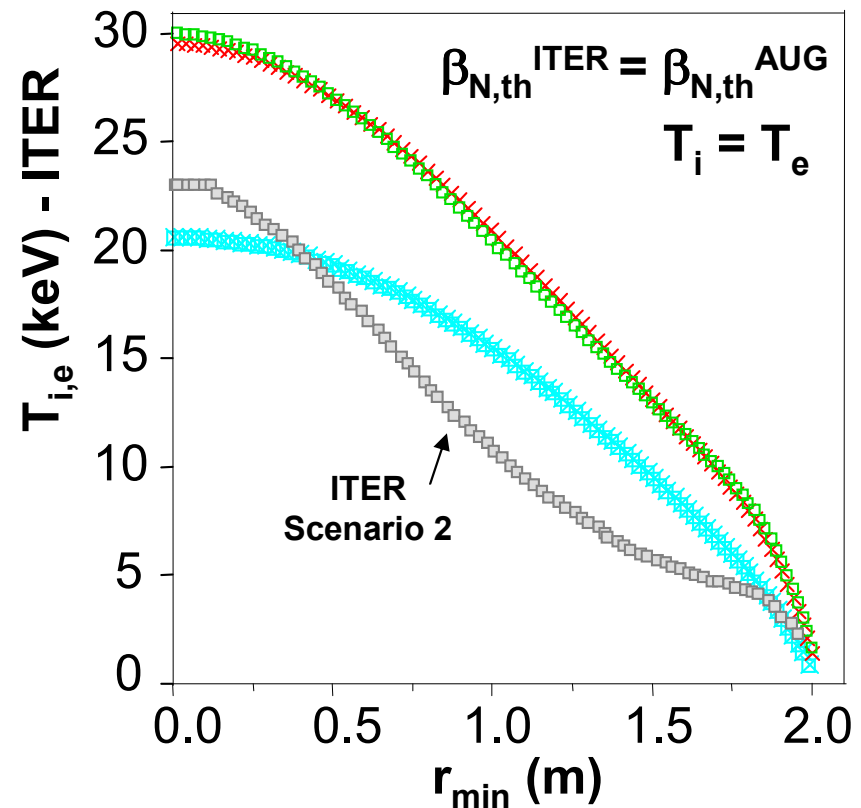
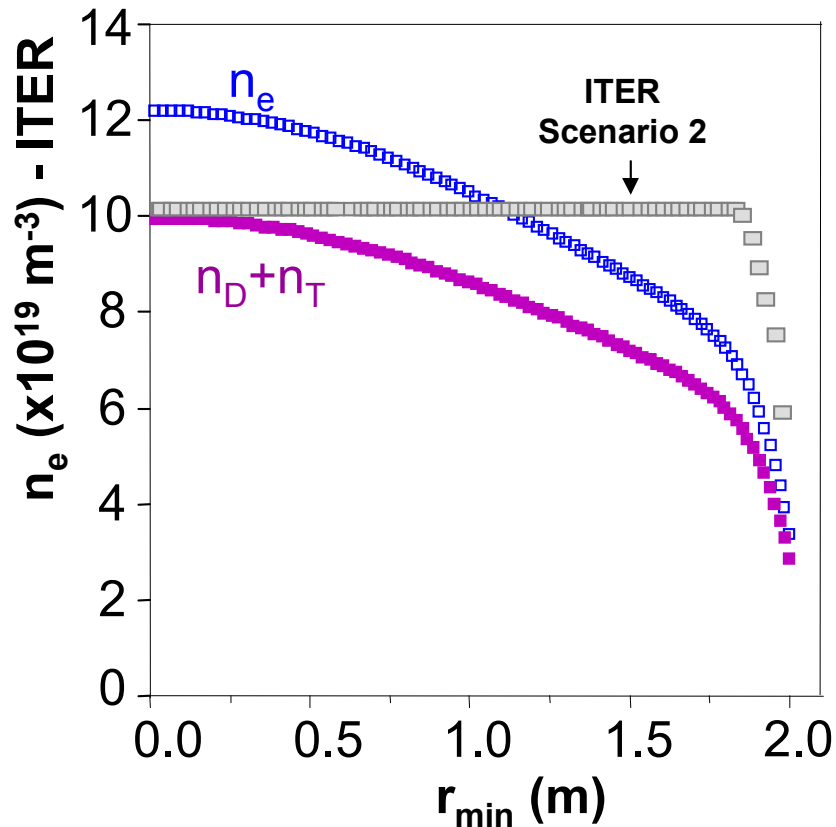
Density: Use shape of n_e profile from ASDEX Upgrade, **set $\langle n_e \rangle = 0.85n_{\text{GW}}$.**

Temperatures: Use shape of T_i profile or use shape of T_e profile from ASDEX Upgrade (select highest), **set $T_i = T_e$ and $\beta_N^{\text{ITER}} = \beta_N^{\text{AUG}}$.**



Comparison with integrated ITER scenario modelling (Scenario 2):

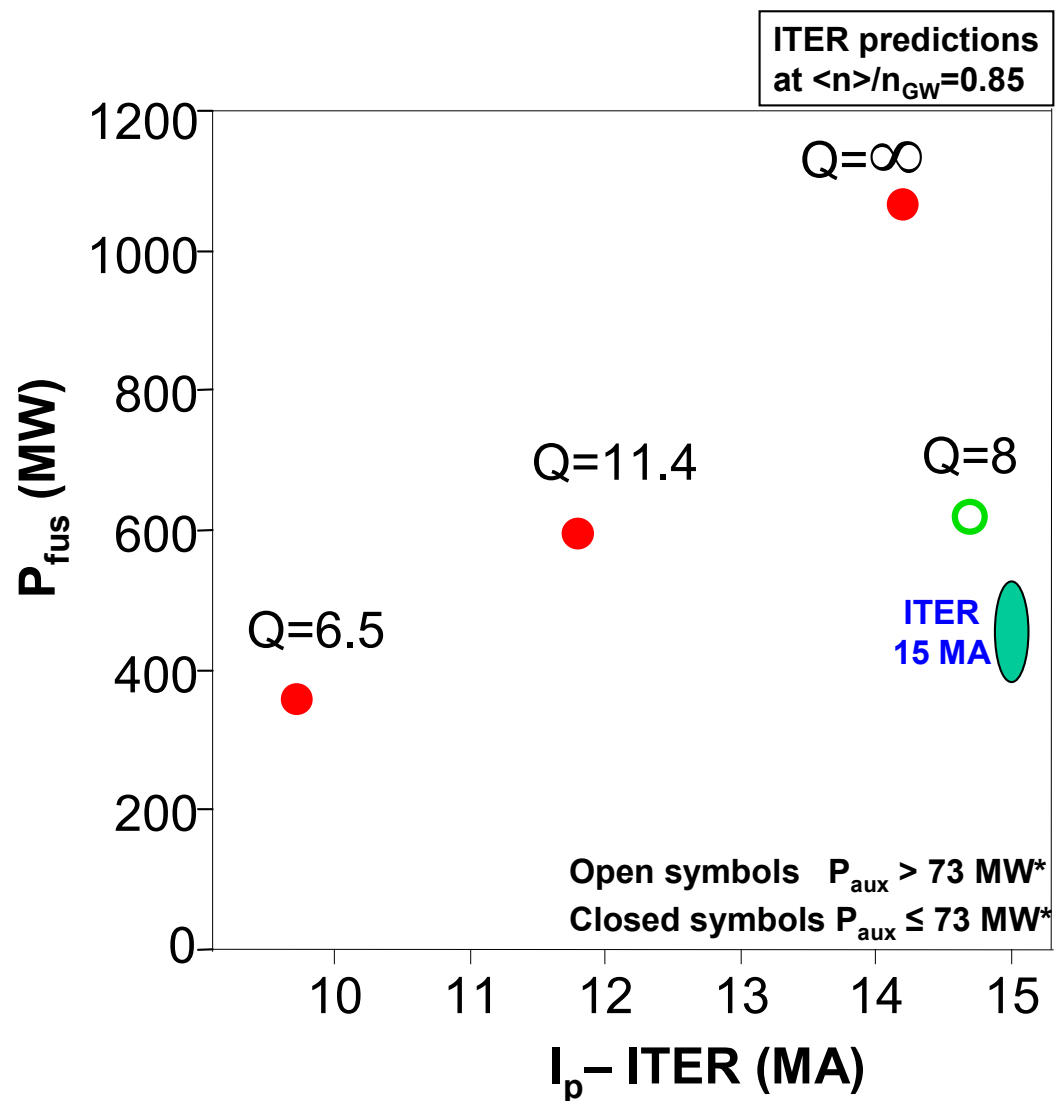
- **Density:** Assumed flat.
- **Temperatures:** Set pedestal, models for core transport & heating systems.



At higher β_N (Improved H-mode):

- Temperature profiles rise over whole plasma region.
- Consistent with observations of increased edge pedestal.

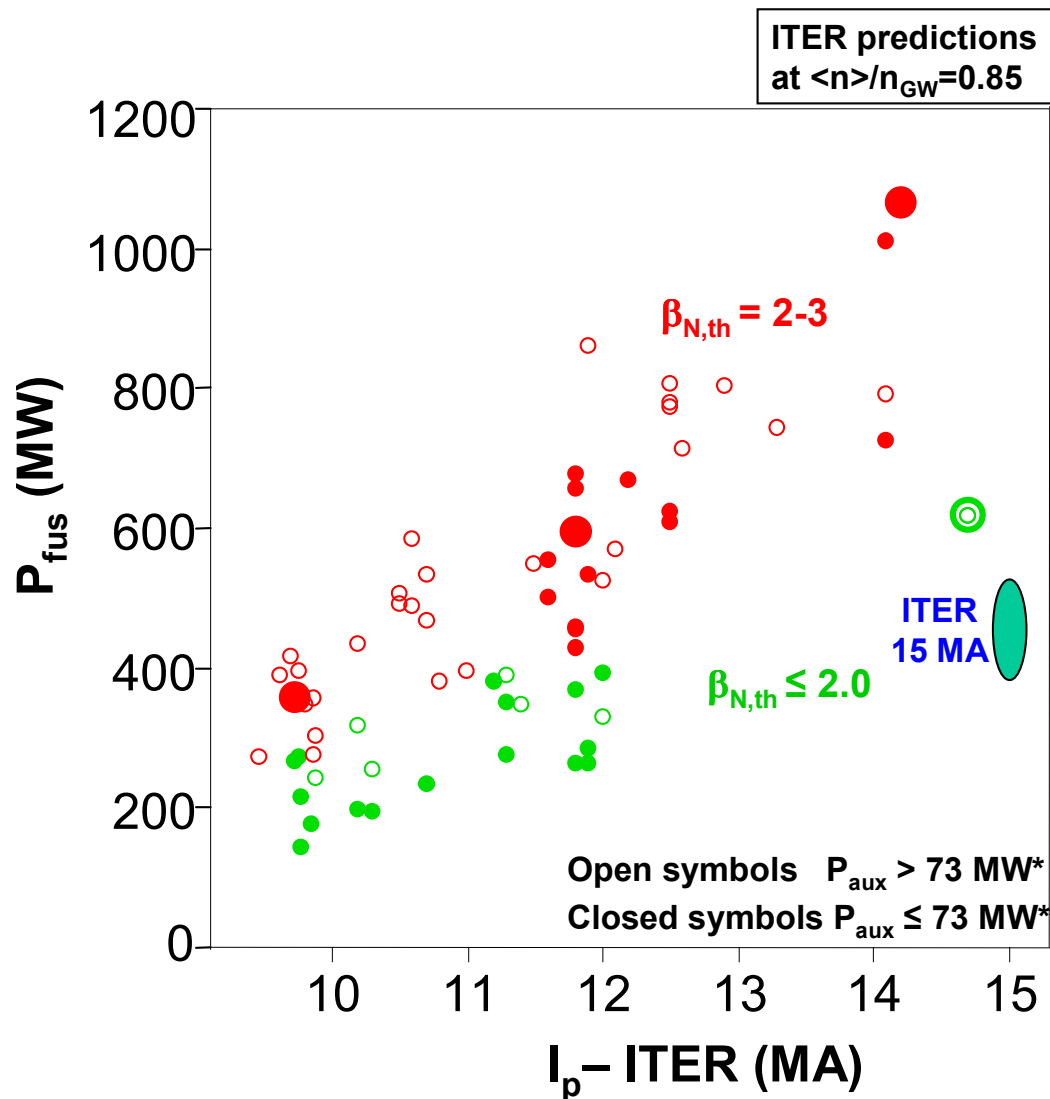
Suttrop W. et al, EX/8-5
Maggi C. et al, IT/P1-6



4 typical cases:

q_{95}	β_N	$H_{98}(y,2)$
3.05	2.10	0.95
3.17	2.87	1.40
3.8	2.63	1.32
4.6	2.41	1.44

* P_{aux} based on using IPB98(y,2) scaling.



Operation at $\beta_{N,th} = 2-3$:

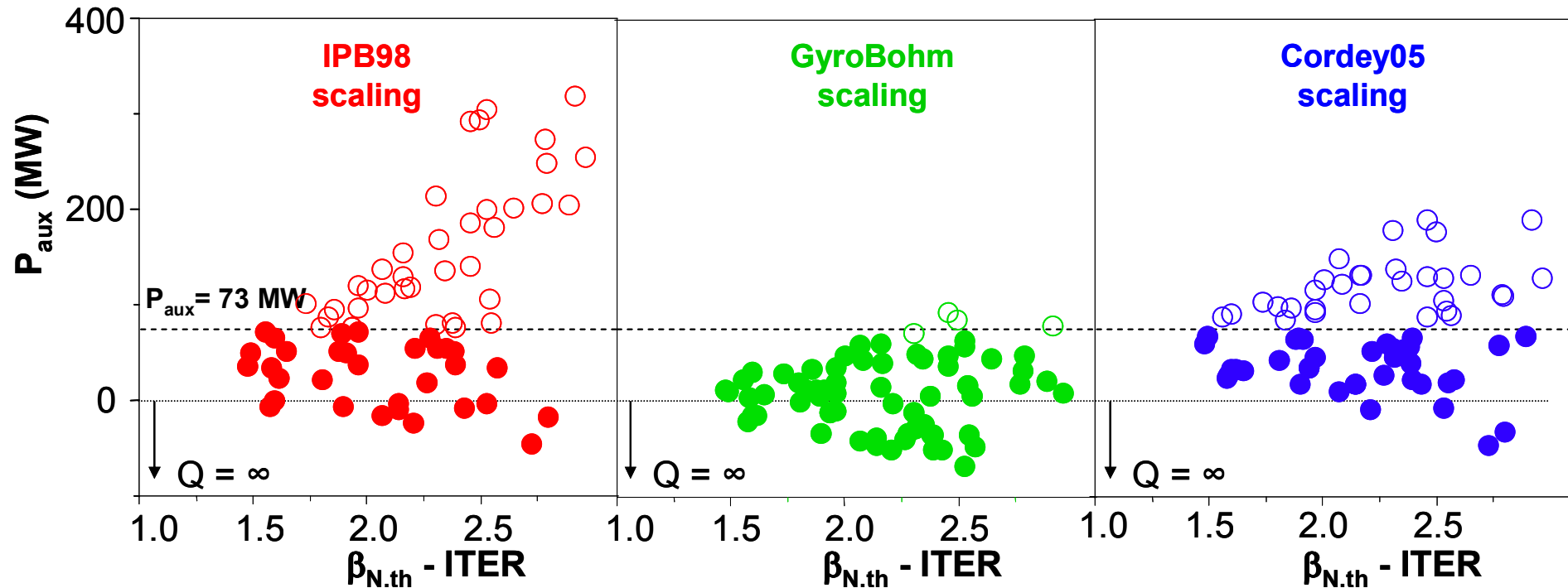
- Significant fusion power for $I_p = 9.5 \text{ MA}$ to $I_p = 12 \text{ MA}$. With bootstrap current fraction $f_{BS} \sim 0.4$, and $Q = 6-15$. Long pulse lengths ($> 400 \text{ s}$).
- At low $q_{95} \sim 3$ ($I_p = 14-15 \text{ MA}$) would in principle be able to reach $P_{fus} \sim 1 \text{ GW}$, $Q = \infty$.

* P_{aux} based on using IPB98(y,2) scaling.

*ITER Physics Basis 1999
Nucl. Fusion 39 2137*

*Petty G. et al 2003
Fusion Sci. Technol. 43 1*

*Cordey J. G. et al 2005
Nucl. Fusion 45 1078*



Q and input power (P_{aux}) required (ASDEX Upgrade profile data):

- Calculated for three different energy confinement scaling expressions.
- Using IPB98(y,2): In some high β cases : $P_{aux} > 73$ MW.
 $I_p < 11$ MA, despite $H_{98}(y,2) \sim 1.4$.

ASDEX Upgrade:

H-modes with low magnetic shear in the centre: $H_{98}(y,2) > 1$ and $\beta_N=2-3.5$.

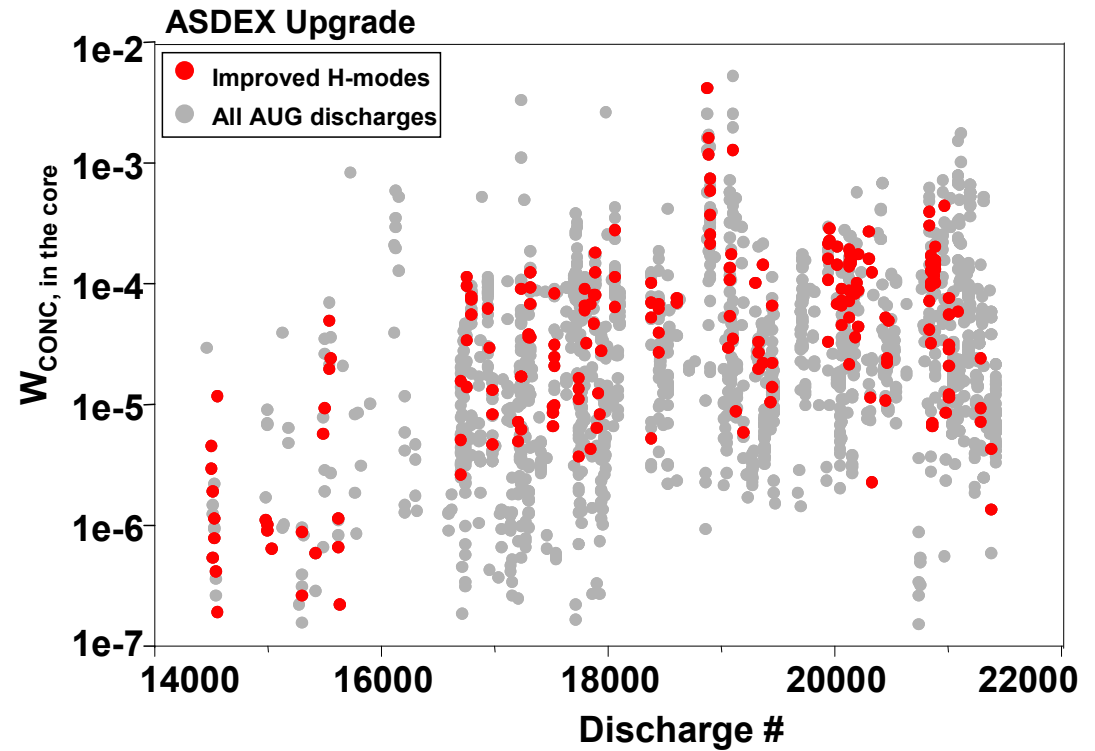
- Operation at high density and $T_{i0}/T_{e0} \sim 1$ is demonstrated.
- Highest $H_{98}(y,2)$ values are achieved at ITER relevant v^* .
- At $q_{95}=3.1$: $H_{98}(y,2)=1.4$, $\beta_N=2.9$, fishbone activity keeps $q(r)$ stationary.
- ECCD can be used to stabilise (3,2) NTM activity ($q_{95} \sim 3$).

ITER predictions, scaling kinetic profile shapes : $\langle n_e \rangle = 0.85 n_{GW}$, keep $\beta_{N,th}$.

At $q_{95}=3.1$: $P_{fus}=1070$ MW, $Q=\infty$.

At $I_p=9.5-12$ MA: P_{fus} 300-600 MW, $Q=6-15$ (some cases $P_{aux}>73$ MW).

Back-up slides

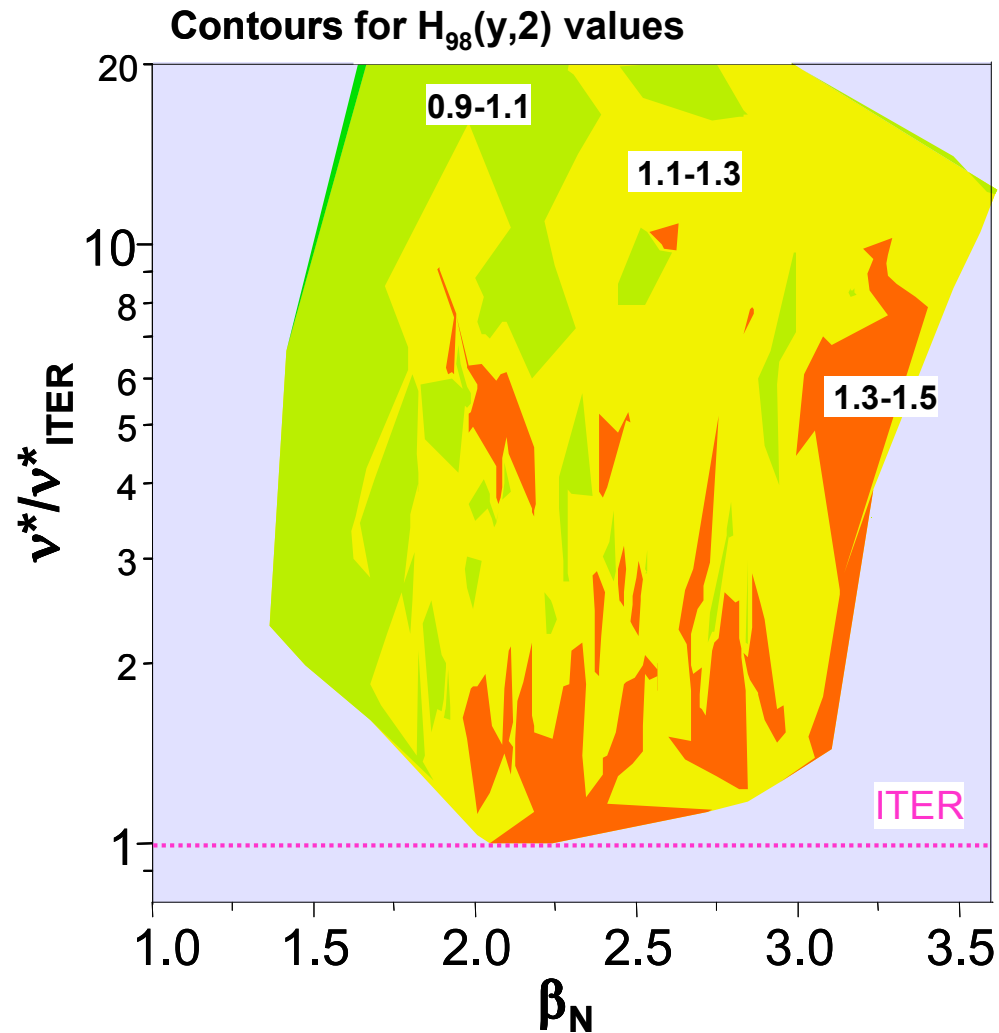


All H-modes require central ICRH or ECRH to avoid impurity accumulation.

Operation at $\langle n_e \rangle \sim 4\text{-}6 \times 10^{19} \text{ m}^{-3}$ requires a boronisation to minimise tungsten influxes.

Gruber O. et al, OV/2-3

Dux R. et al, EX/3-3Ra



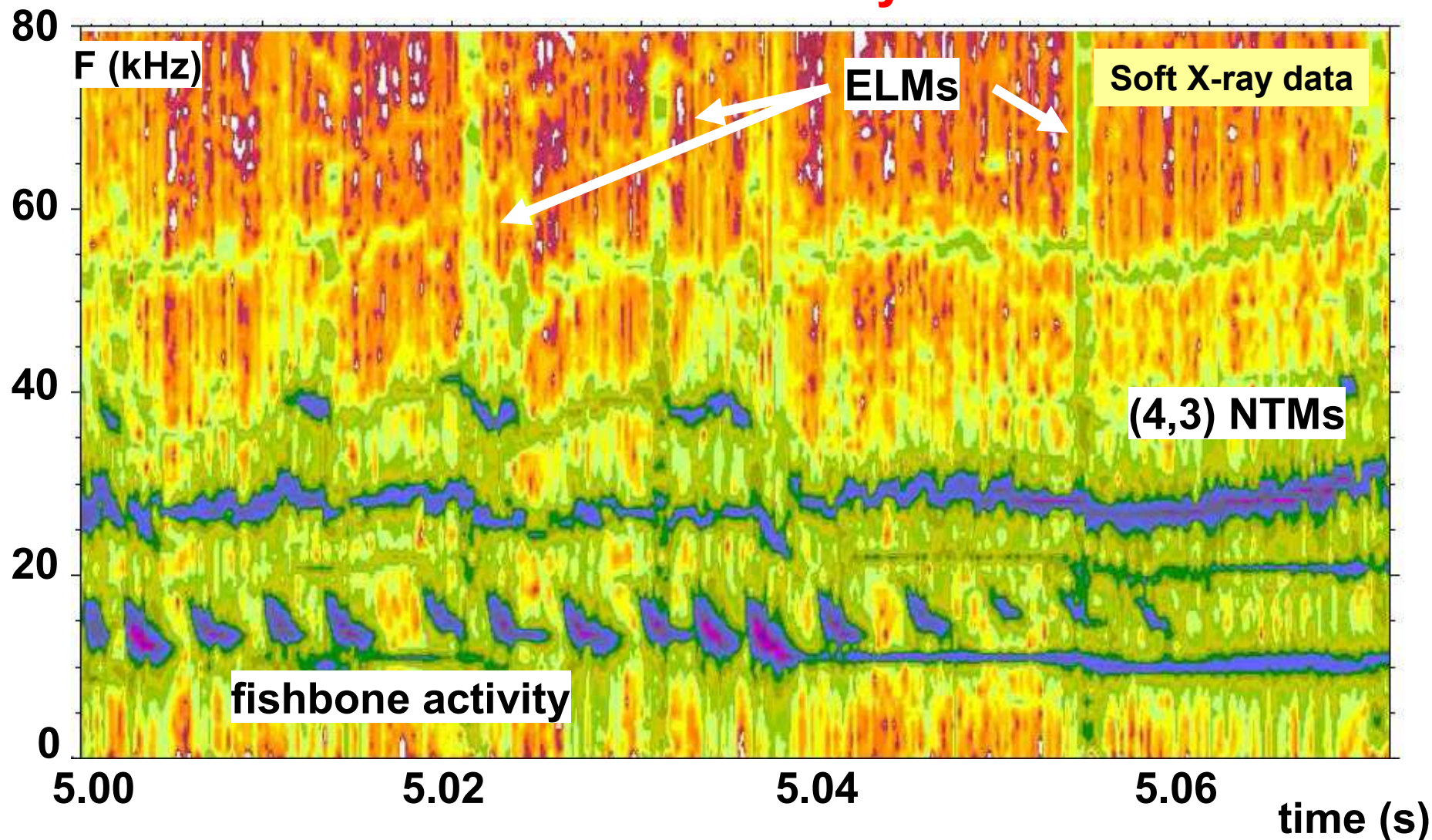
Strongest correlation of maximum $H_{98}(y,2)$ with plasma collisionality (v^*/v_{ITER}^*).

Also density peaking ($n_{e0}/\langle n_e \rangle$) can be higher at lower v^*/v_{ITER}^* .

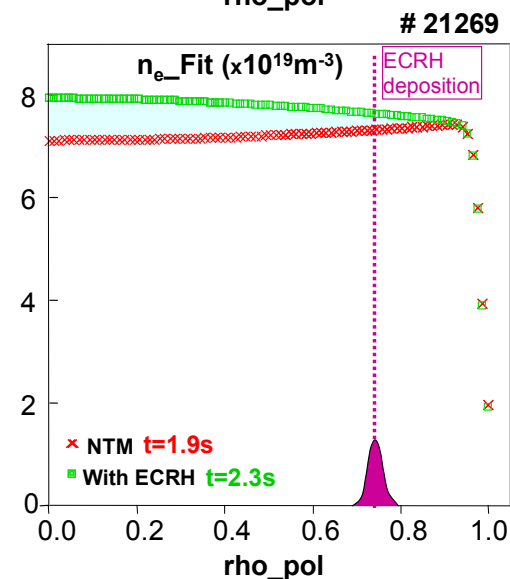
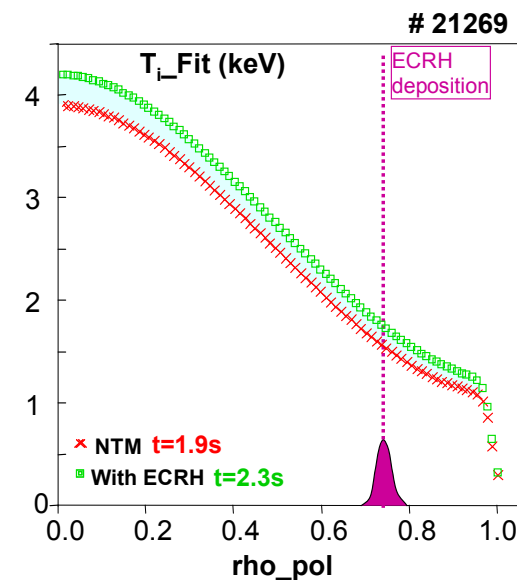
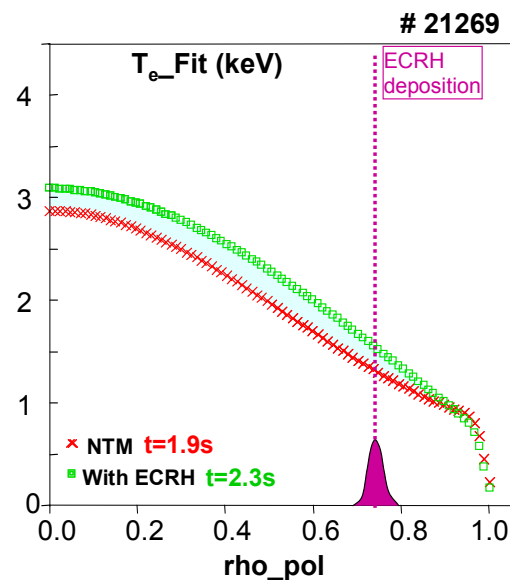
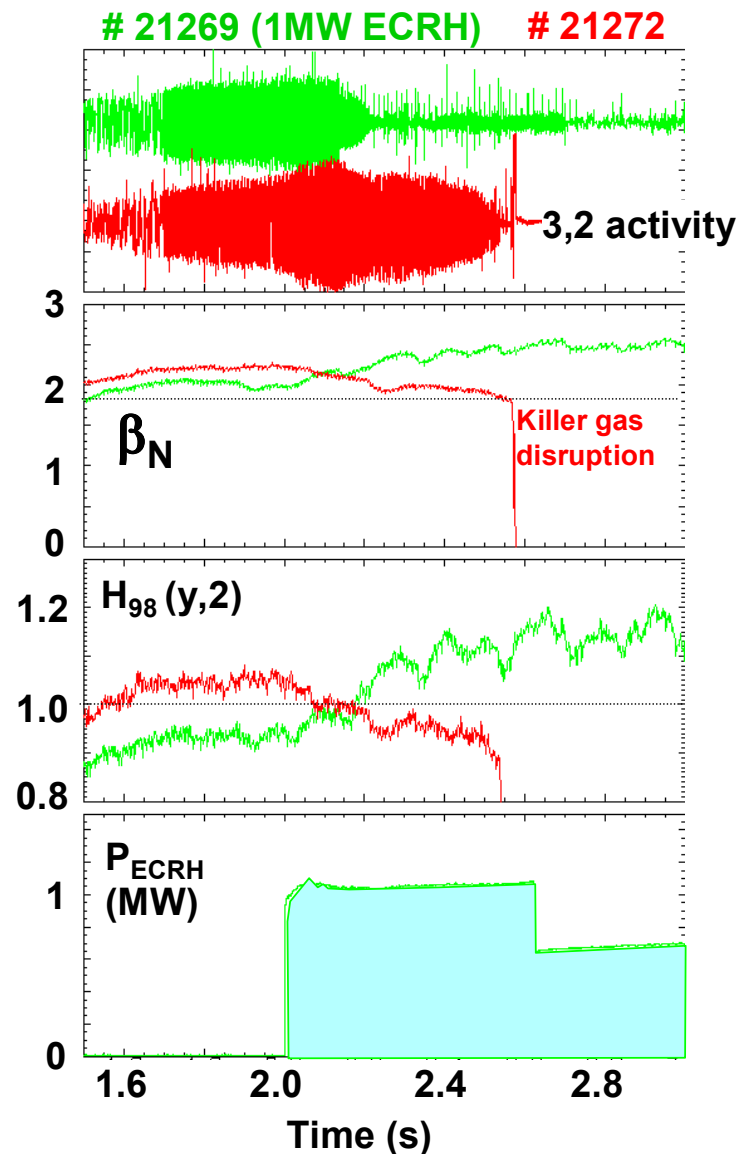
→ β and v^* dependence of the IPB98(y,2) scaling expression are under investigation.

McDonald D. et al, EX/P3-5

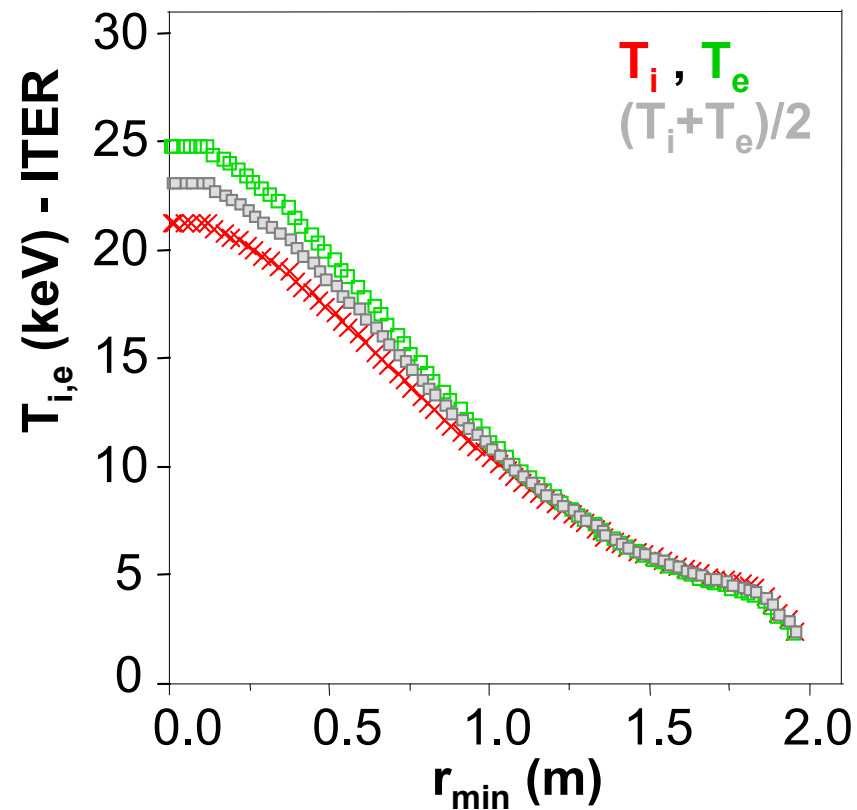
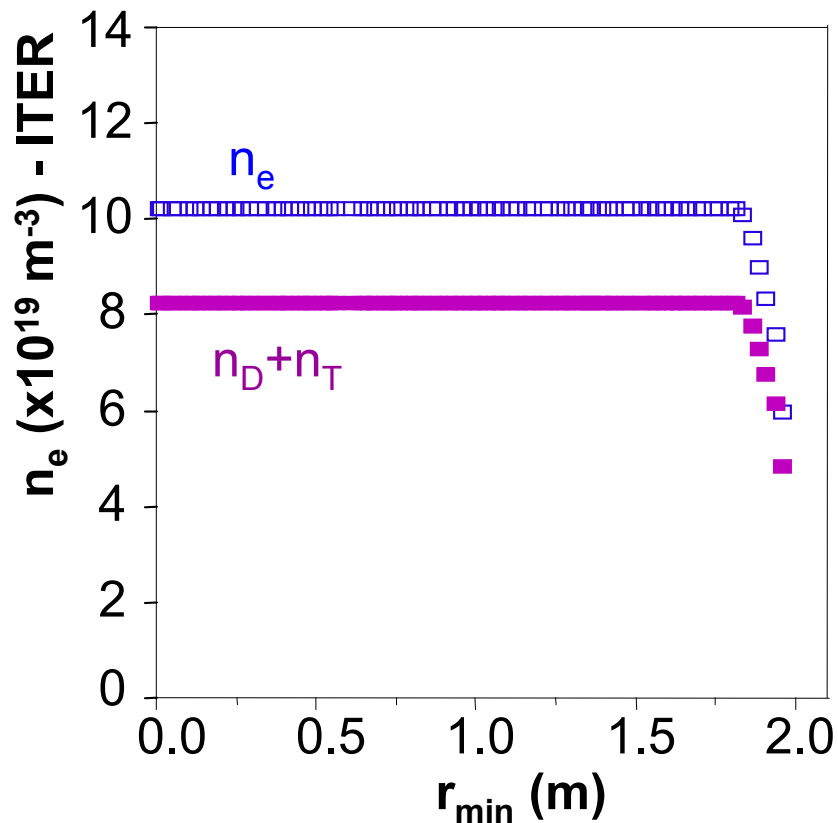
Core MHD activity



Use of ECRH to stabilise (3,2) NTM

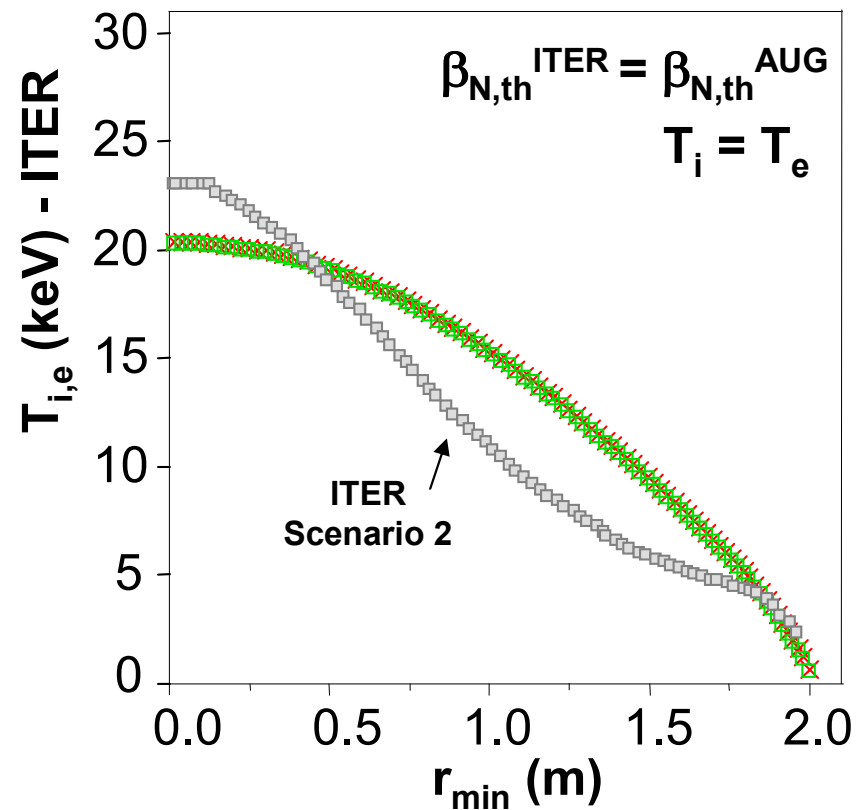
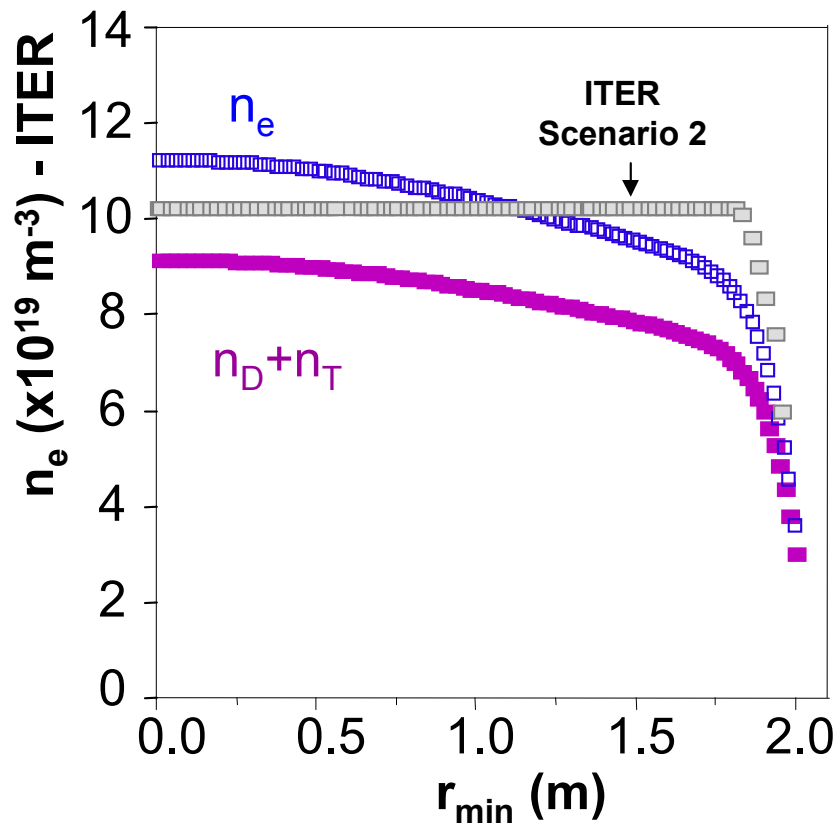


Zohm H. et al, EX/4-1Rb

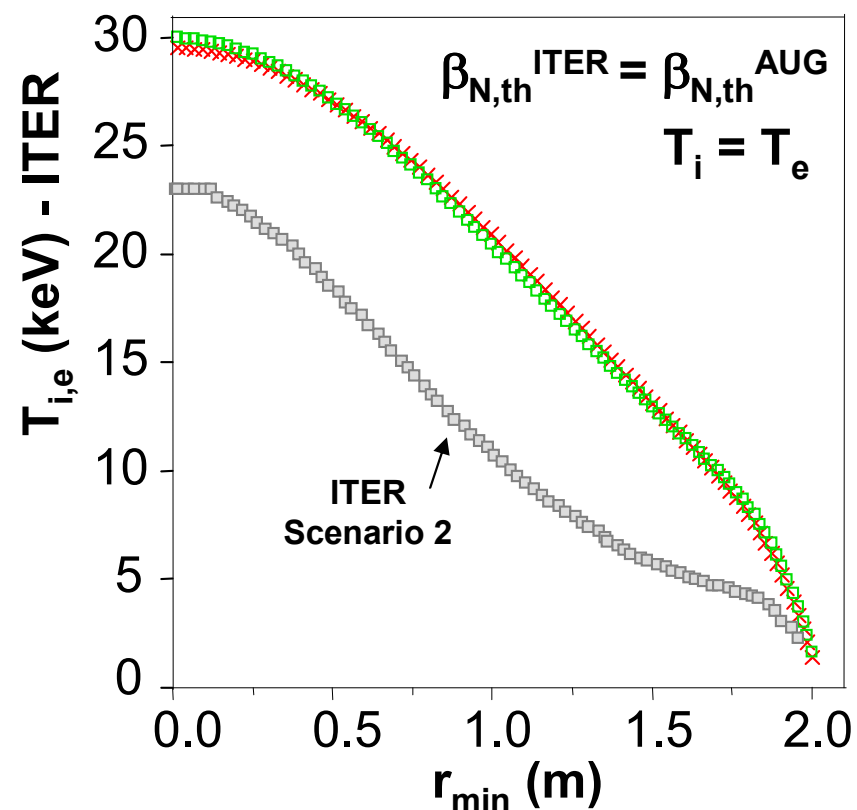
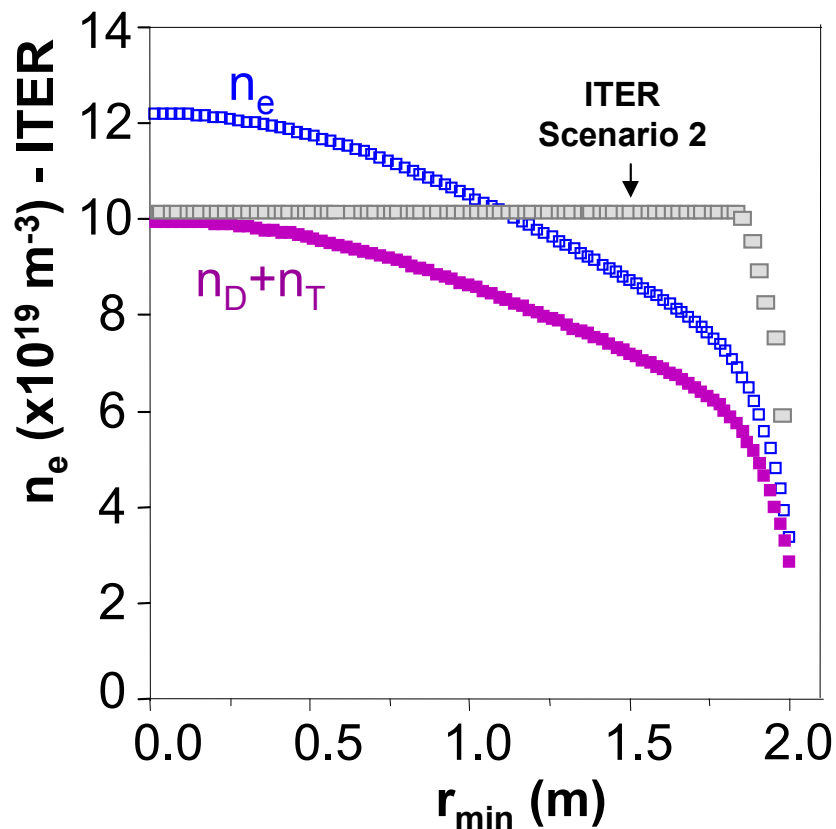


$\langle n_e \rangle / n_{\text{GW}} = 0.85$	q_{95}	I_p (MA)	β_N	P_{fus} (MW)	$H_{98}(y,2)$	Q	P_{aux} (MW)	$\langle n_e \rangle$ (10^{19} m^{-3})	n_{e0} (10^{19} m^{-3})	T_{e0}/T_{i0} (keV)
ITER Sc. 2	3.0	15.0	1.8	400	1.0	10	40	10.1	10.2	24.8/ 21.2

Scaling to ITER: $q_{95}=3.0$, $\beta_N=2.1$, high $\langle n_e \rangle$

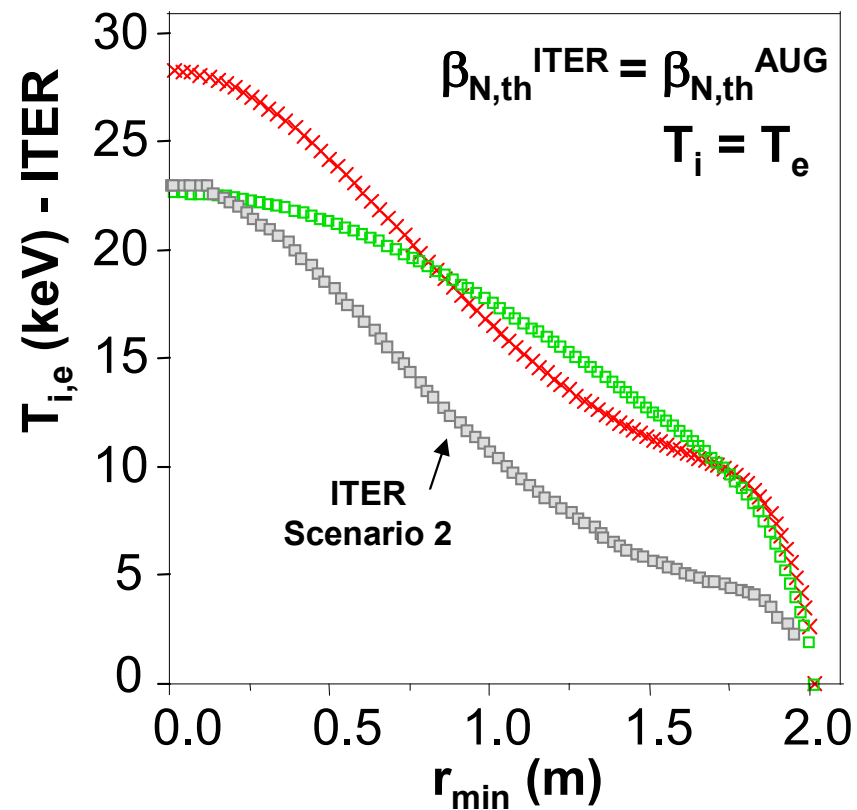
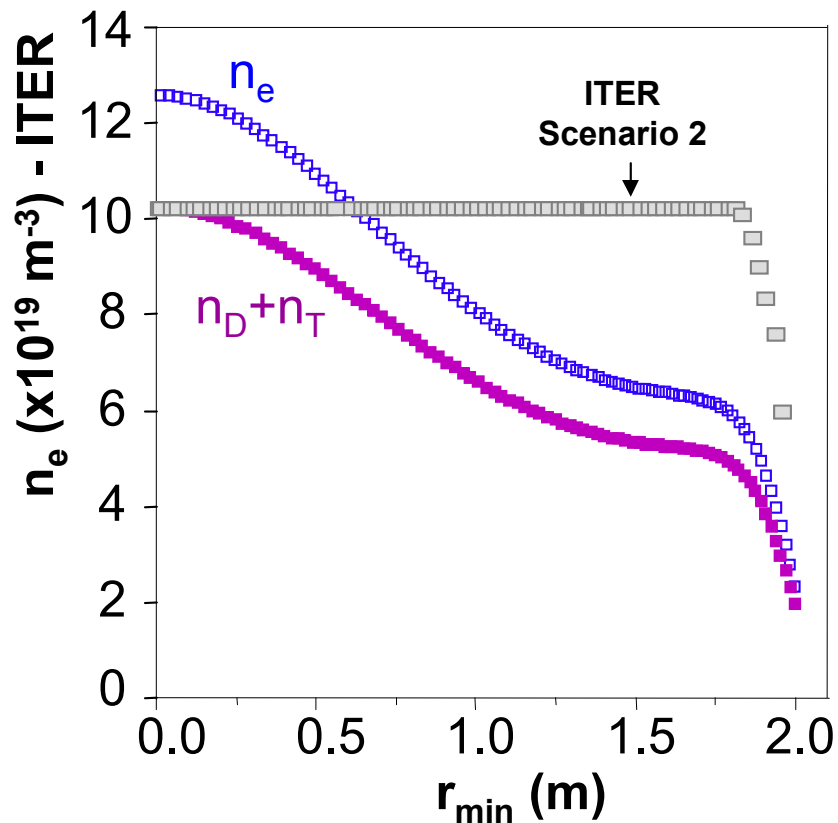


$\langle n_e \rangle / n_{GW}$ = 0.85	q_{95}	I_p (MA)	β_N	P_{fus} (MW)	$H_{98}(y,2)$	Q	P_{aux} (MW)	$\langle n_e \rangle$ ($10^{19}m^{-3}$)	n_{e0} ($10^{19}m^{-3}$)	T_{e0}/T_{i0} (keV)
AUG #17847	3.05	14.7	2.10	619	0.95	8.0	(78)	9.9	11.2	20.3



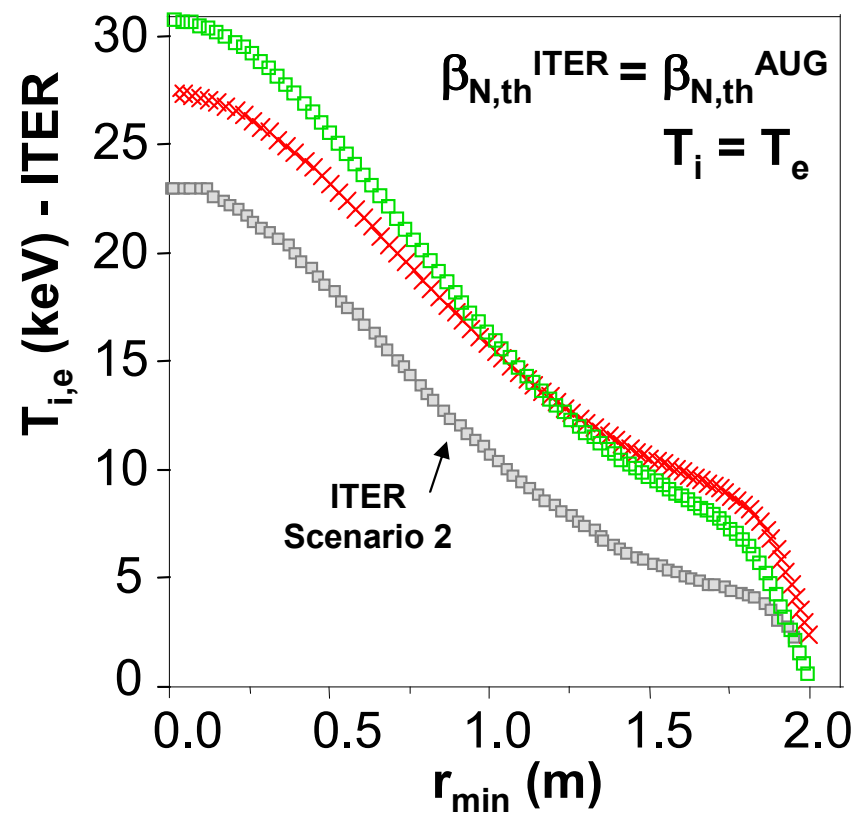
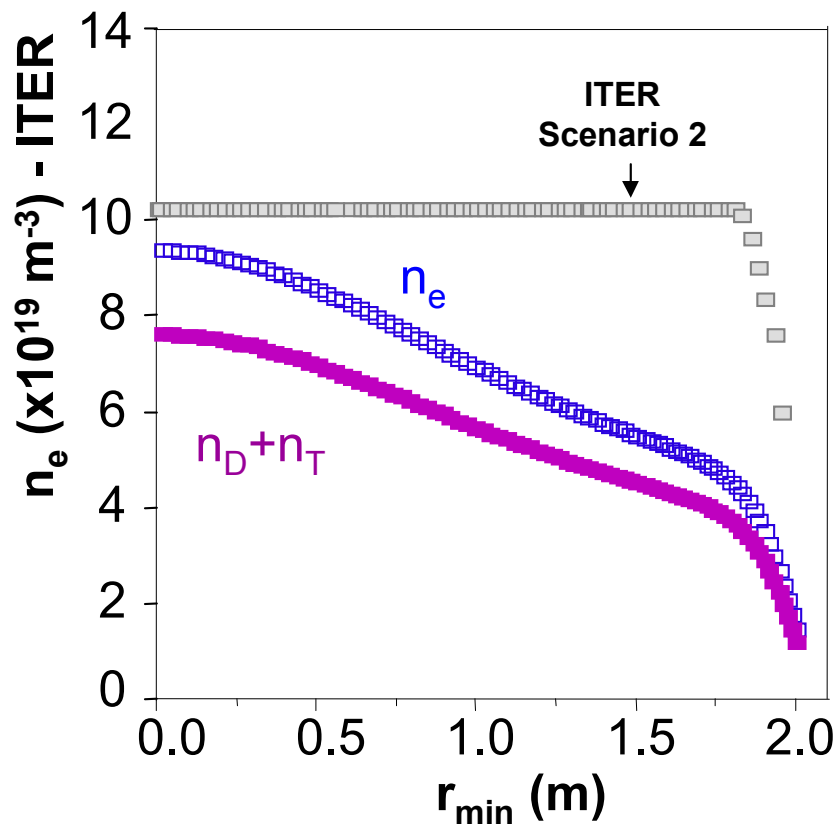
$\langle n_e \rangle / n_{GW}$ = 0.85	q_{95}	I_p (MA)	β_N	P_{fus} (MW)	$H_{98}(y,2)$	Q	P_{aux} (MW)	$\langle n_e \rangle$ ($10^{19}m^{-3}$)	n_{e0} ($10^{19}m^{-3}$)	T_{e0}/T_{i0} (keV)
AUG #20449	3.17	14.2	2.87	1070	1.40	∞	0	9.6	12.2	29.5

Scaling to ITER: $q_{95}=3.8$, $\beta_N=2.6$



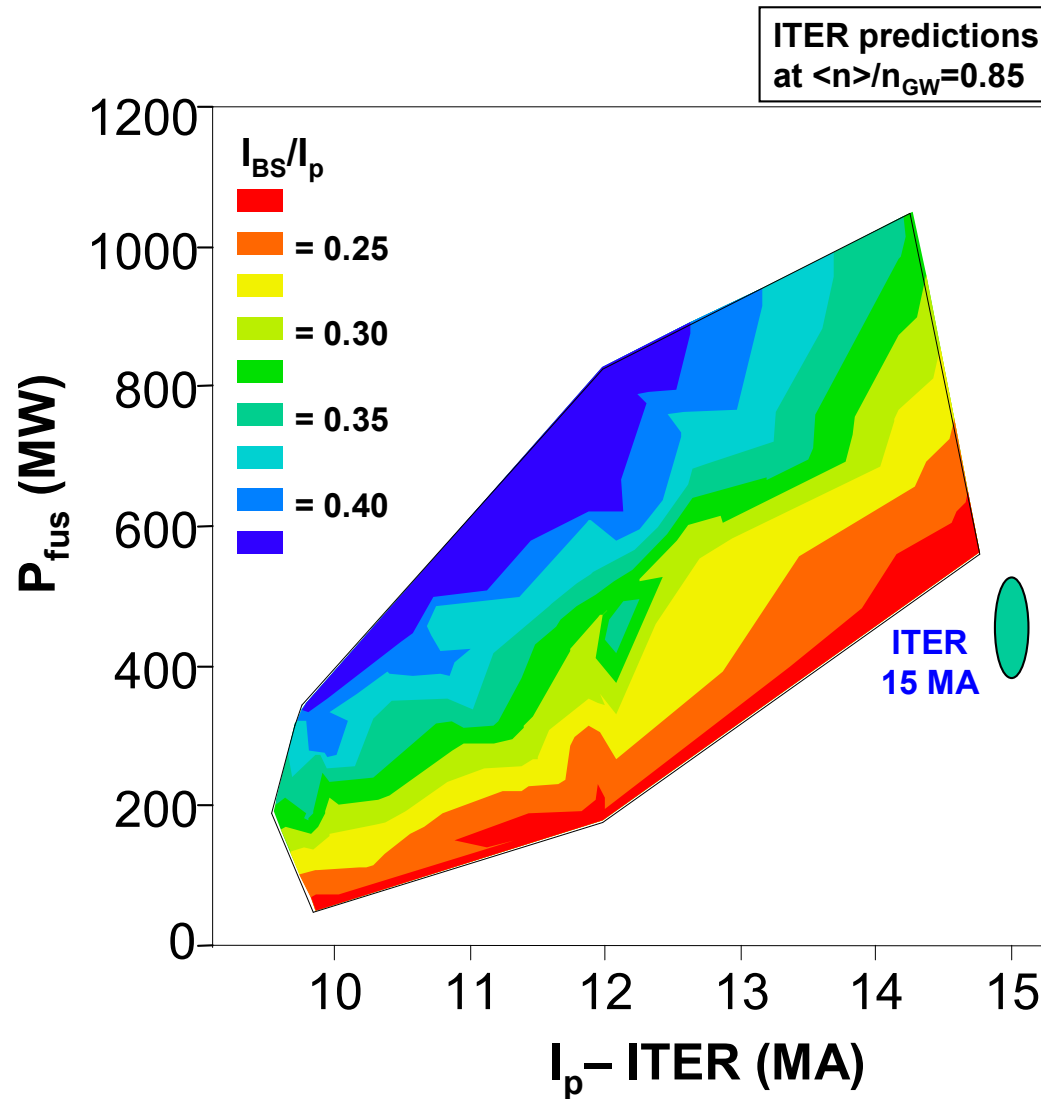
$\langle n_e \rangle / n_{\text{GW}} = 0.85$	q_{95}	I_p (MA)	β_N	P_{fus} (MW)	$H_{98}(y,2)$	Q	P_{aux} (MW)	$\langle n_e \rangle$ (10^{19} m^{-3})	n_{e0} (10^{19} m^{-3})	T_{e0} / T_{i0} (keV)
AUG #17870	3.8	11.8	2.63	597	1.32	11.4	52	8.0	12.6	28.2

Scaling to ITER: $q_{95}=4.6$, $\beta_N=2.4$



$\langle n_e \rangle / n_{GW}$ = 0.85	q_{95}	I_p (MA)	β_N	P_{fus} (MW)	$H_{98}(y,2)$	Q	P_{aux} (MW)	$\langle n_e \rangle$ ($10^{19}m^{-3}$)	n_{e0} ($10^{19}m^{-3}$)	T_{e0}/T_{i0} (keV)
AUG #20448	4.6	9.7	2.41	360	1.44	6.5	55	6.6	9.4	27.4

$\langle n_e \rangle / n_{GW} = 0.85$	q_{95}	I_p (MA)	β_N	P_{fus} (MW)	$H_{98}(y,2)$	Q	P_{aux} (MW)	$\langle n_e \rangle$ ($10^{19}m^{-3}$)	n_{e0} ($10^{19}m^{-3}$) profile shapes	T_{e0}/T_{i0} (keV)
ITER Sc. 2	3.0	15.0	1.8	400	1.0	10	40	10.1	10.2	24.8/ 21.2
AUG #17847	3.05	14.7	2.10	619	0.95	8.0	(78)	9.9	11.2	20.3
AUG #20449	3.17	14.2	2.87	1070	1.40	∞	0	9.6	12.2	29.5
AUG #17870	3.8	11.8	2.63	597	1.32	11.4	52	8.0	12.6	28.2
AUG #20448	4.6	9.7	2.41	360	1.44	6.5	55	6.6	9.4	27.4



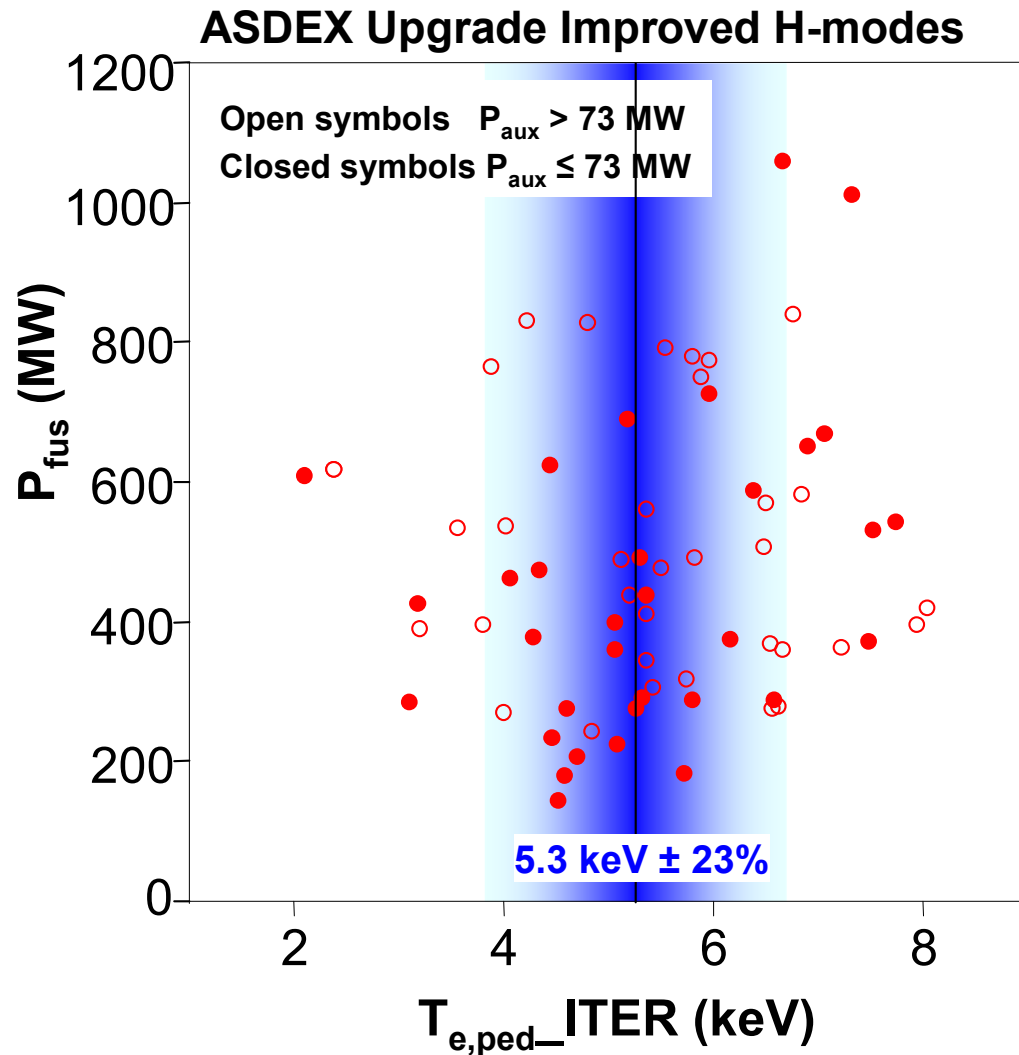
Calculated bootstrap fraction f_{BS} increases at lower current.

ITER (15MA) ~ 0.18 .

Maximum of cases presented here: $f_{BS} \sim 0.4$.

A current ramp to lower plasma currents compared to reference design AND the ability to operate at same stored energy.

\rightarrow longer pulse length.



Most of the scaled edge pedestal temperatures are within range of what is expected for typical H-modes in ITER.

$5.3 \text{ keV} \pm 23\%$

*Sugihara M. et al 2003
 Plasma Phys. Control.
 Fusion 45 L55*